Applied Mathematics and Computation 368 (2020) 124584

Contents lists available at ScienceDirect

Applied Mathematics and Computation

journal homepage: www.elsevier.com/locate/amc

Stability analysis and control strategies for worm attack in mobile networks via a VEIQS propagation model

Qingwu Gao [a,b,*], Jun Zhuang [b]

[a] School of Statistics and Mathematics, Nanjing Audit University, Nanjing, China
[b] Department of Industrial and Systems Engineering, University at Buffalo, Buffalo, USA

ARTICLE INFO

Article history:
Received 18 January 2019
Revised 4 July 2019
Accepted 8 July 2019

Keywords:
Mobile-networks based worm
Saturated incidence rate
Vaccination
Quarantine
Basic reproduction number
Equilibria

ABSTRACT

Mobile devices are considerably pervasive in society, but also increase their vulnerability to worm attacks from mobile networks. In this paper, we propose a new Vulnerable-Exposed-Infectious-Quarantined-Secured worm propagation model with saturated incidence and strategies of both vaccination and quarantine. We obtain that the basic reproduction number R_0 is a sharp threshold parameter such that the worm-free equilibrium is asymptotically stable for $R_0 \leq 1$, implying that the worm dies out eventually and its attack remains under control; the worm-existence equilibrium is asymptotically stable when $R_0 > 1$, namely, the worm is always persistent and spreading within a population. This paper provides some novel insights to cyber security by that (a) the stability of worm-free equilibrium establishes the control strategies to reduce the intensity of worm attacks, and the optimal control strategy is proposed by using Pontryagins Minimum Principle; (b) the stability of worm-existence equilibrium predicts the tendency of worm propagation in a long run and assesses the level of the worm popularity by the final scale of infected devices. Numerical simulations are implemented to illustrate the feasibility of the theoretical results and the effectiveness of the control strategies.

1. Introduction

In today's world, mobile devices (e.g., smartphone, laptop, and tablet) have been increasingly pervasive and considerably facilitated our daily life. For example, a smartphone can access a large variety of services, including surfing the web, online shopping or banking, mobile payment, and instant messaging. However, the services provided by these mobile devices increase their risks of exposure to worm attacks from mobile networks, such as the ones based on Bluetooth, SMS/MMS and Internet access. In high-speed networks, malicious worms breakout and spread fast due to their sophisticated spreading mechanisms. The time taken for the infection of global targets has shrunk from days to minutes [1]. Meanwhile, the majority of mobile devices have not been designed to guard against worm attacks, making them vulnerable to such attacks and then become an attractive target and victim for worms. In 2004, the first Bluetooth-based worm, named Cabir, was launched. Once two Bluetooth-enabled devices are in range, the compromised device pairs with its target using default passwords and then sends malicious contents [2]. In 2008, Commwarrior, a SMS/MMS-based worm which delivers malicious content and maintains communication with an attacker, appeared on the Internet [3]. The malicious worms can rapidly infect millions of

* Corresponding author at: School of Statistics and Mathematics, Nanjing Audit University, Nanjing, China.
E-mail addresses: qwgao@aliyun.com, qingwuga@buffalo.edu (Q. Gao).

https://doi.org/10.1016/j.amc.2019.124584
0096-3003/

mobile devices and bring huge economic losses [4,5]. A new Wi-Fi worm, called Chameleon, which could spread in a manner similar to that of airborne diseases, appeared in 2014 [6]. If a mobile device has been compromised by the worms based on Internet access, it may cause great disruption to its user, including data leakage, system damage, financial losses, and privacy leakage [7]. Hence, the outbreak of malicious worms is considered by network experts as one of the most critical threats to cyber security, functionality, and assets.

It is a research topic of considerable interest not only to accurately model the dynamic behavior of the worm propagation in mobile networks, but also to effectively fight against this worm prevalence among mobile devices. In the past decades, researchers have proposed many mathematical models by ordinary differential equations (ODEs), see [8–12] and the references therein. An important quarantine strategy was taken into account in the DQ model [13], PWDQ model [14], SEIQV model [15,16], SEIQRS model [17], and SEIQR model [18]. The Internet access station (e.g., Wi-Fi base station) could easily quarantine infectious devices by cutting off their connection to other devices [18], which can save the susceptible devices from the attack of worms. Also in [19], the process of protecting devices from infection by vaccination has substantial historical success in reducing both morbidity and mortality. Due to the high similarity between network worms and biological viruses, vaccination by installing efficient antivirus software or immunization procedures has been an effective defense mechanism to control the attack of worms, and the vaccination is assumed to have full efficacy and permanent immunity [15,16,20,21]. But in reality, the efficacy of such software does not reach 100% [22,23]. Thus, this research aims at an ODE worm propagation model with both the quarantine strategy for infectious devices and the vaccination strategy towards vulnerable devices, where an imperfect vaccine effectiveness is considered.

The studies on epidemic models for biological viruses and network worms have demonstrated that the incidence rate plays a critical role to describe the virus transmission or the worm propagation, where a bilinear incidence rate is frequently used [9,11,15,17,18,23]. However, the bilinear incidence rate appears unrealistic so that it limits the usefulness of obtained results in most practical situations. Then, many nonlinear incidence rates of more general forms have been proposed [16,24–28]. The saturated incidence rate, a nonlinear incidence rate, tends to a saturation level as the number of susceptible devices increases or the number of infectious devices gets larger. This incidence rate is more reasonable than the bilinear incidence rate because it includes the inhibition effect from the behavioral change of susceptible devices and the crowding effect of the infectious devices, and also prevents the unboundedness of contact rate by choosing suitable parameters, which, clearly, can reduce the intensity of worm attack. In this study, an ODE mathematical model with the saturated incidence rate is developed to simulate more accurately the dynamic behavior of the worm propagation and to effectively mitigate the worm attack in mobile networks.

Inspired by the above-mentioned references, we propose a new VEIQS (Vulnerable-Exposed-Infectious-Quarantined-Secured) worm propagation model with the saturated incidence rate, which focuses on the dynamics of the worm propagation and the control strategies for worm attack by mitigating its magnitude and speed. The novel idea in the proposed model is to combine both vaccination and quarantine strategies. In comparison to the existing results, the topological structures of the VEIQS model may be very complex, and then the theoretical analysis has considerable difficulty to some extent. Using the basic reproduction number, the local and global stabilities in both the worm-free and worm-existence equilibria are derived, along side efficient worm-epidemic control strategies for the worm attacks. An optimal control strategy (or impulse control) is also considered to minimize the systemic cost of vaccination and quarantine as well as minimize the infected mobile devices and maximize the secured devices. It is worth emphasizing that the stability for the worm-free equilibrium is the theoretical basis of these control strategies; and the stability for the worm-existence equilibrium can give a prediction of the tendency of worm propagation in a long run, and can obtain the final scale of infected devices (including exposed, infectious, and quarantined devices). Meanwhile, some numerical simulations are carried out to illustrate the feasibility of our theoretical results and the effectiveness of the obtained control strategies.

The remaining part of this paper is organized as follows: Section 2 proposes a new VEIQS worm propagation model with a saturated incidence rate and security countermeasures; Section 3 presents the stability analysis of the worm-free and worm-existence equilibria; Section 4 covers the numerical analysis and the simulation; Section 5 gives the optimal control strategy and some other control strategies to mitigate of worm attacks; Section 6 concludes the paper with future research directions. The corresponding proofs of this study are available in Appendix.

2. VEIQS worm propagation model

Recently, Xiao et al. [18] developed an SEIQR (Susceptible-Exposed-Infectious-Quarantined-Recovered) worm propagation model, which describes the dynamic behaviors and characteristics of the worm spreading in a Wi-Fi environment. An effective quarantine strategy was also presented to control the prevalence of the Wi-Fi-based worms. But in practice, the scenario described in the SEIQR model does not coincide with a real mobile network. Particularly, there are two problematical issues. Firstly, mobile devices can access the Web not only via Wi-Fi networks but also via other Internet access; e.g., 4G networks. Then, Internet access including Wi-Fi networks and 4G networks should be considered as one of the most widely used means to connect to the mobile Internet among the mobile devices. Secondly, besides the quarantine strategy, the vaccination strategy with antivirus treatment is usually employed to protect from the worm propagation among mobile devices and decrease the intensity of worm attacks in mobile networks. Also, the effects of other control strategies are analyzed on the exposed and infectious states to prevent worm propagation in a short period immediately after detecting the worm attack, which greatly mitigates the possibility of worm outbreak in early stage among mobile devices.

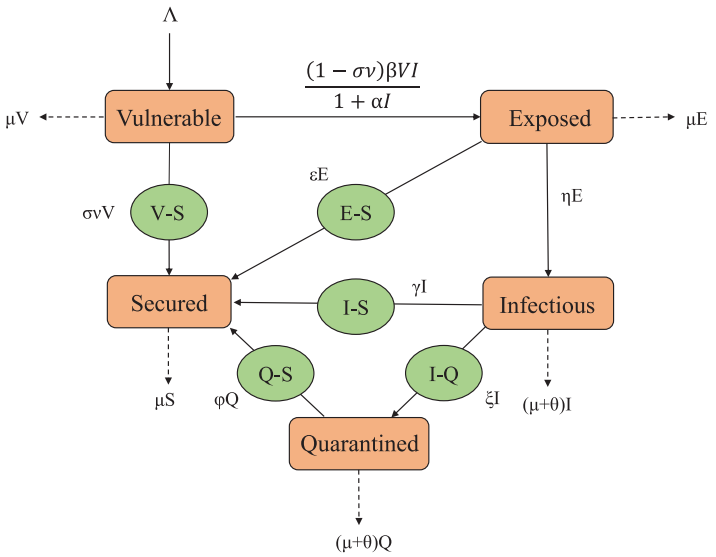

Fig. 1. State transition diagram of the VEIQS model.

The SEIQR model only adopted the concept of natural death, and dysfunction occurs in all susceptible, exposed, infectious, quarantined, and recovered states. However, the majority of mobile devices crash due to the attack of malicious worms, so the more abnormal functioning of devices arises in the infectious and quarantined states which contain mobile devices infected by these malicious worms. Furthermore, the SEIQR model is accompanied with the bilinear incidence rate, which appears far too unrealistic in most practical situations to achieve the usefulness of obtained results. This paper analyzes a worm propagation model with the saturated incidence rate, a more reasonable nonlinear incidence rate, to consider the crowding effect of the infectious devices and prevent the unboundedness of the contact rate by choosing suitable parameters, where the saturated incidence rate can be used to reduce the intensity of worm attack.

The arguments above motivate us to develop a more suitable VEIQS model, where we take information terminology and control strategies into account for mobile devices to prevent the worm propagation in mobile networks and further defend against the worm attacks among mobile devices. Thus, we use the state names, "vulnerable" instead of "susceptible", and "secured" instead of "recovered". The states of mobile devices are defined as follows: Vulnerable state (V) includes those devices which are vulnerable to worm attacks in mobile networks, but have not been infected by the malicious worm; Exposed state (E) includes those devices which are exposed to the attacks and have been infected, but not actively infectious due to the latent time requirement; Infectious state (I) includes those exposed devices which are actively searching and targeting new victims; Quarantined state (Q) includes those infectious devices which are quarantined by the Internet access station; Secured state (S) includes those devices which gained one or more security countermeasures, providing the devices with a permanent immunity against the malicious worms. The block diagram of VEIQS model state transition and model parameters involved are shown in Fig. 1. Table 1 shows notation used in this paper and baseline parameter values used in Section 4. Table 2 shows a summary of the state transitions and rates of devices in the VEIQS model.

Combining Fig. 1, Tables 1 and 2, the state transitions of devices in VEIQS model are detailed as follows:

1. Using vaccination strategy via antivirus treatment in V-state to improve their immunity capability to control worm attack, vulnerable devices can be vaccinated at a vaccine coverage rate of ν $(0 \le \nu < 1)$. Due to the partial efficiency of the vaccine, only σ $(0 \le \sigma \le 1)$ fraction of the vaccinated vulnerables, namely $\sigma\nu V$ vulnerable devices in all, move to the S-state, where σ $(0 \le \sigma \le 1)$ represents the vaccine efficacy. When $\sigma = 0$, the vaccination strategy has no effect at all; when $\sigma = 1$, the vaccination strategy is perfectly effective.
2. The remaining $(1-\nu)$ fraction of vulnerable devices and the remaining $(1-\sigma)$ fraction of vaccinated vulnerables both have no immunity to worm attacks, and then have to go to the E-state. In other words, $\frac{(1-\sigma\nu)\beta VI}{1+\alpha I}$ (i.e., $\frac{(1-\nu)\beta VI}{1+\alpha I} + \frac{(1-\sigma)\nu\beta VI}{1+\alpha I}$) vulnerable devices transition to the E-state, where $\frac{\beta VI}{1+\alpha I}$ denotes the saturated incidence rate, $\frac{\beta I}{1+\alpha I}$ tends to a saturation level when I gets larger, βI measures the infection force when the worm is entering a fully vulnerable population, and $\frac{1}{1+\alpha I}$ measures the inhibition from the crowding effect of the infectious devices and prevents the unboundedness of the contact rate by choosing suitable parameters.
3. The exposed devices transit into infectious state with rate η when the worm begins actively scanning the networks for new victims, where $1/\eta$ is the mean latent period. As $\eta \to \infty$, the latent period becomes negligible, and the VEIQS model degenerates to a VIQS model.

Table 1
Notation and parameter values in the model.

Notation	Explanation	Initial values
$N(t)$	Total number of devices at time t	N(0)=75,000
$V(t)$	Number of vulnerable devices at time t	Not fixed
$E(t)$	Number of exposed devices at time t	Not fixed
$I(t)$	Number of infectious devices at time t	Not fixed
$Q(t)$	Number of quarantined devices at time t	Q(0)=0
$S(t)$	Number of secured devices at time t	S(0)=0
Λ	Recruitment rate	0.75
μ	Natural death rate	0.00001
θ	Worm-related death rate	0.001
σ	Vaccination effective rate	0.6
ν	Vaccination coverage rate	Not fixed
α	Constant parameter in saturated incidence rate	0.8
β	Infection rate of vulnerable devices by infectious devices	0.053
η	State transition rate from E to I	0.008
ϵ	State transition rate from E to S	0.0008
γ	State transition rate from I to S	0.05
ξ	State transition rate from I to Q	0.05
φ	State transition rate from Q to S	0.005

Table 2
State transition events and transition rates.

Events including intermediate control strategies	Rate of transition
V $\rightarrow$ E	$(1\text{-}\sigma\nu)\beta V(t)I(t)/(1+\alpha I(t))$
V $\rightarrow$ S	$\sigma\nu V(t)$
E $\rightarrow$ I	$\eta E(t)$
E $\rightarrow$ S	$\epsilon E(t)$
I $\rightarrow$ Q	$\xi I(t)$
Q $\rightarrow$ S	$\varphi Q(t)$
V $\rightarrow$ Dysfunctional	$\mu V(t)$
E $\rightarrow$ Dysfunctional	$\mu E(t)$
I $\rightarrow$ Dysfunctional	$(\mu+\theta)I(t)$
Q $\rightarrow$ Dysfunctional	$(\mu+\theta)Q(t)$
S $\rightarrow$ Dysfunctional	$\mu S(t)$
Replaced $\rightarrow$ V	Λ

4. Considering the quarantine strategy imposed in the I-state, the infectious devices can be quarantined into the Q-state with a quarantine rate ξ. When $\xi = 0$, the quarantine strategy is not considered and no infectious device is quarantined. Thus the VEIQS model degenerates to a VEIS model [21,23,27].
5. Using some sufficient defense mechanisms, a portion of the exposed, infectious, and quarantined devices in the networks become secured with an acquired permanent immunity, at rates ε, γ, and φ, respectively. The constant $1/\varphi$ is the mean quarantine period. As $\varphi \rightarrow \infty$, the quarantine period becomes negligible, and then the VEIQS model degenerates to a VEIS model [21,23,27].
6. Device dysfunction occurs in all states because of the natural death, but more importantly, the dysfunction mainly arises in the states I and Q due to the attacks of malicious worms. The replacement of dysfunctional devices is done in V-state and its rate in the total devices is denoted by Λ.

Compared to the existing literature, the proposed VEIQS model combines worm-epidemic control strategies to prevent the worm propagation in mobile networks and reduce the intensity of worm attacks to mobile devices, and also evaluates the effect of these strategies on all the states except the S-state. As shown in Fig. 1, the recovery routes for states V, E, I, and Q are designed to estimate the recovery rate for each state in a real network worm attack. From the recovery routes, we consider the control measures as follows:

1. The recovery route from V-state (V-S) is obtained from the vaccination strategy taken in the V-state to prevent the attack of worms.
2. The recovery route from E-state (E-S) is obtained from a certain control measure taken in the E-state after detecting the worm attack.
3. The recovery route from I-state (I-S) is obtained from a control measure taken in I-state after the worm became active.
4. Another recovery route from I-state (I-Q) is obtained from the quarantine strategy taken in I-state to quarantine infectious devices by the Internet access station.
5. The recovery route from Q-state (Q-S) is obtained from the security countermeasure taken in Q-state after the infectious devices are quarantined.

Based on the statements above, the VEIQS model with a saturated incidence rate and control strategies can be formulated by the following non-linear ODEs:

$$\begin{cases} V'(t) = \Lambda - \dfrac{(1-\sigma\nu)\beta VI}{1+\alpha I} - (\sigma\nu+\mu)V, \\ E'(t) = \dfrac{(1-\sigma\nu)\beta VI}{1+\alpha I} - (\eta+\epsilon+\mu)E, \\ I'(t) = \eta E - (\xi+\gamma+\mu+\theta)I, \\ Q'(t) = \xi I - (\varphi+\mu+\theta)Q, \\ S'(t) = \sigma\nu V + \epsilon E + \gamma I + \varphi Q - \mu S. \end{cases} \tag{1}$$

Let $N(t)$ be the total number of mobile devices at time t, which satisfies

$$N(t) = V(t) + E(t) + I(t) + Q(t) + S(t).$$

Note that $N(t)$ varies with time since mobile devices enter and leave the system either through migration, natural death or worm-induced death, which imbalances the inflows and outflows of a given system. Summing the equations in (1) gives

$$N'(t) = \Lambda - \mu N - \theta(I+Q) \le \Lambda - \mu N.$$

After a simple computation, we have

$$N(t) \le \left(N(0) - \frac{\Lambda}{\mu}\right)e^{-\mu t} + \frac{\Lambda}{\mu},$$

and then

$$\lim_{t\to\infty} N(t) = \frac{\Lambda}{\mu},$$

which means that $N(t)$ approaches to the stable equilibrium point Λ/μ as $t\to\infty$. Denote the feasible region of system (1) by

$$\Omega = \left\{(V,E,I,Q,S) \in \mathbb{R}^5_+ | 0 \le V+E+I+Q+S \le \frac{\Lambda}{\mu}\right\}.$$

To enrich the plausibility of our VEIQS model proposed by system (1), we need to make non-negativity analysis. In fact, the first equation of (1) implies that

$$V'(t) \le \Lambda - (\sigma\nu+\mu)V,$$

which leads to

$$V(t) \le \frac{\Lambda}{\sigma\nu+\mu} + \left(V(0) - \frac{\Lambda}{\sigma\nu+\mu}\right)e^{-(\sigma\nu+\mu)t}.$$

For a long time, we have

$$V(t) \le \frac{\Lambda}{\sigma\nu+\mu} =: \Delta_1.$$

This, along with the second equation of (1), yields that

$$E'(t) \le \frac{(1-\sigma\nu)\beta\Delta_1}{\alpha} - (\eta+\epsilon+\mu)E,$$

It follows that

$$E(t) \le \frac{(1-\sigma\nu)\beta\Delta_1}{\alpha(\eta+\epsilon+\mu)} + \left(E(0) - \frac{(1-\sigma\nu)\beta\Delta_1}{\alpha(\eta+\epsilon+\mu)}\right)e^{-(\eta+\epsilon+\mu)t},$$

which, for a long time, shows that

$$E(t) \le \frac{(1-\sigma\nu)\beta\Delta_1}{\alpha(\eta+\epsilon+\mu)} =: \Delta_2.$$

By the similar derivations as above, we still obtain that

$$I(t) \le \frac{\eta\Delta_2}{\xi+\gamma+\mu+\theta} = \Delta_3,$$

$$Q(t) \le \frac{\xi\Delta_3}{\varphi+\mu+\theta} = \Delta_4,$$

$$S(t) \leq \frac{\sigma\nu\Delta_1 + \epsilon\Delta_2 + \gamma\Delta_3 + \varphi\Delta_4}{\mu}.$$

Hence from the above discussion, we obtain the following proposition.

Proposition 1. *The solutions of system (1) with initial conditions satisfy $V(t) > 0$, $E(t) > 0$, $I(t) > 0$, $Q(t) > 0$, and $S(t) > 0$ for all $t > 0$, and the feasible region Ω is a positively invariant and attracting set with respect to system (1).*

3. Stability analysis

In this section, we firstly present the worm-free and worm-existence equilibria and the basic reproduction number of the VEIQS model proposed in this paper. Secondly, we provide the local and global stabilities of the worm-free equilibrium, which establish the theoretical basis of the control strategies for worm attacks. Thirdly, we explore the uniform persistence of system (1). Finally, the local and global stabilities of the worm-existence equilibrium are in detail analyzed to predict the tendency of the worm propagation in a long run and to measure the level of the popularity of worm attacks by the final scale of the infected devices (including exposed, infectious, and quarantined devices).

3.1. Equilibria and basic reproduction number

The basic reproduction number, denoted by R_0, is a fundamental concept in epidemic dynamics of biological diseases and network worms, which refers to "the average number of secondary cases generated by one primary case at the start of the epidemic in a completely susceptible population" [29,30]. And the number R_0 essentially determines the dynamic behavior of an epidemic and how intensive a policy will need to be to control the epidemic [30].

According to the theory of the next generation operator [31], we determine the expression for the number R_0. Firstly, we establish the worm-free equilibrium, where the total number of the infected devices, namely, $E(t) + I(t) + Q(t)$, tends to 0 as the time t goes to infinity. Then it is easy to obtain that the system (1) always has the worm-free equilibrium:

$$P_0 = (V_0, E_0, I_0, Q_0, S_0) = \left(\frac{\Lambda}{\sigma\nu + \mu}, 0, 0, 0, \frac{\sigma\nu}{\mu}V_0\right). \tag{2}$$

Let $E'(t) = \frac{(1-\sigma\nu)\beta VI}{1+\alpha I} - (\eta + \epsilon + \mu)E = 0$, we have $E = \frac{(1-\sigma\nu)\beta V_0 I}{(1+\alpha I)(\eta+\epsilon+\mu)}$, where $V_0 = \frac{\Lambda}{\sigma\nu+\mu}$. Thus,

$$\begin{aligned}\mathbf{D}_I(I'(t)) &= \mathbf{D}_I\left[\frac{(1-\sigma\nu)\beta\eta\Lambda I}{(1+\alpha I)(\eta+\epsilon+\mu)(\sigma\nu+\mu)} - (\xi+\gamma+\mu+\theta)I\right] \\ &= \frac{(1-\sigma\nu)\beta\eta\Lambda}{(\sigma\nu+\mu)(\eta+\epsilon+\mu)}\frac{1}{(1+\alpha I)^2} - (\xi+\gamma+\mu+\theta),\end{aligned}$$

and then at $I_0 = 0$,

$$A = D_I\,|_{I=I_0} = \frac{(1-\sigma\nu)\beta\eta\Lambda}{(\sigma\nu+\mu)(\eta+\epsilon+\mu)} - (\xi+\gamma+\mu+\theta) =: M - D$$

Subsequently, we obtain the basic reproduction number R_0 as

$$R_0 = \frac{M}{D} = \frac{(1-\sigma\nu)\beta\eta\Lambda}{(\sigma\nu+\mu)(\eta+\epsilon+\mu)(\xi+\gamma+\mu+\theta)}. \tag{3}$$

In fact, the basic reproduction number can also be derived with the method of next generation matrix [29]. To study the dynamic behavior of the VEIQS model described by system (1), we now present the following results on the worm-free and worm-existence equilibria.

Theorem 1. *When $R_0 \leq 1$, the worm-free equilibrium P_0 is the only equilibrium in Ω of the form (2); when $R_0 > 1$, the unique worm-existence equilibrium $P^* = (V^*, E^*, I^*, Q^*, S^*)$ exists in* int(Ω) *with coordinates satisfying*

$$\begin{cases} I^* = \dfrac{(1-\sigma\nu)\beta\eta\Lambda - (\sigma\nu+\mu)(\eta+\epsilon+\mu)(\xi+\gamma+\mu+\theta)}{(\eta+\epsilon+\mu)(\xi+\gamma+\mu+\theta)[(1-\sigma\nu)\beta + \alpha(\sigma\nu+\mu)]}, \\ V^* = \dfrac{(\eta+\epsilon+\mu)(\xi+\gamma+\mu+\theta)(1+\alpha I^*)}{(1-\sigma\nu)\beta\eta}, \\ E^* = \dfrac{\xi+\gamma+\mu+\theta}{\eta}I^*, \\ Q^* = \dfrac{\xi}{\varphi+\mu+\theta}I^*, \\ S^* = \dfrac{\sigma\nu V^* + \epsilon E^* + \gamma I^* + \varphi Q^*}{\mu}. \end{cases} \tag{4}$$

Also, $N^* = V^* + E^* + I^* + Q^* + S^*$.

Remark 1. The worm-existence equilibrium with its coordinates (V^*, E^*, I^*, Q^*, S^*) can give the final scales of the vulnerable, exposed, infectious, quarantined, and secured devices, respectively, as the time t tends to infinity. In particular, the final scale of infected devices, i.e., $E^* + I^* + Q^*$, can be used to measure the level of the worm popularity.

Note here that the basic reproduction number R_0 is a sharp threshold parameter that determines the existence of the worm-free and worm-existence equilibria. For the proof of Theorem 1, refer to Appendix A1.

3.2. Stability of worm-free equilibrium

In the subsection, we present two theorems regarding the dynamic behavior of the worm-free equilibrium. See Appendixes A2 and A3 for their proofs. The first theorem is concerned with the local and asymptotical stability.

Theorem 2. *When* $R_0 \le 1$, *the worm-free equilibrium* P_0 *is locally asymptotically stable with respect to* Ω; *otherwise,* P_0 *is unstable.*

Further, we discuss the global and asymptotical stability of the worm-free equilibrium, which, along with Theorem 2, shows that the local and global stabilities are equivalent.

Theorem 3. *When* $R_0 \le 1$, *the worm-free equilibrium* P_0 *is globally asymptotically stable with respect to* Ω; *otherwise,* P_0 *is unstable.*

Remark 2. In Theorems 2 and 3, the local and global stabilities of the worm-free equilibrium P_0 mean that when $R_0 \le 1$, $V(t)$ and $S(t)$ approach to their steady states $\frac{\Lambda}{\sigma\nu+\mu}$ and $\frac{\sigma\nu}{\mu}V_0$, but the infected states (i.e., E_0, I_0, and Q_0) all approach to 0, as the time t goes to infinity, which implies that $R_0 \le 1$ guarantees the worm is dying out in the end and then its attack remains under control. Hence, in order to bring the worm attack under control, we adopt some feasible and effective strategies to reduce R_0 to be less than unity, where these strategies are the control strategies, appearing in Section 5, to reduce the intensity of worm attack. From the arguments above, Theorems 2 and 3 are the theoretical basis of these control strategies.

Note also that the basic reproduction number R_0 not only determines the local and global stabilities of the worm-free equilibrium P_0, but also governs whether the infected devices disappear in time locally and globally, respectively, which implies that the number R_0 will play an important role in the control of an epidemic of worm in mobile networks. See Section 5 for more details.

3.3. Uniform worm persistence

In this subsection, we explore the uniform persistence of system (1) when the basic reproduction number $R_0 > 1$, by the acyclicity theorem [32, P. 18], and its proof is delayed to Appendix A4.

Definition 1. [33] The system (1) is said to be uniformly persistent in Ω, if there exists a constant $0 < c < 1$ such that any solution ($V(t)$, $E(t)$, $I(t)$, $Q(t)$, $S(t)$) of system (1) with initial value ($V(0)$, $E(0)$, $I(0)$, $Q(0)$, $S(0)$) $\in \mathrm{int}(\Omega)$ satisfies

$$\min\left\{\liminf_{t\to\infty} V(t), \liminf_{t\to\infty} E(t), \liminf_{t\to\infty} I(t), \liminf_{t\to\infty} Q(t), \liminf_{t\to\infty} S(t)\right\} \ge c.$$

Theorem 4. *System (1) is uniform persistent in* Ω *if and only if* $R_0 > 1$.

Remark 3. The uniform persistence of (1) in the bounded set Ω is equivalent to the existence of a compact set $K \subset \Omega$ that is absorbing for (1) (see [34]).

3.4. Stability of worm-existence equilibrium

In this subsection, we analyze the asymptotical stability of the worm-existence equilibrium P^*, which is of more importance to investigate than the worm-free equilibrium P_0 from the epidemiological perspective. The proofs of main results are presented in Appendixes A.5 and A6.

Theorem 5. *When* $R_0 > 1$, *the worm-existence equilibrium* P^* *is locally asymptotically stable with respect to* Ω.

As generally acknowledged, the local and asymptotical stability of worm-existence equilibrium P^* may be of no practical significance for a real network system since it merely guarantees this stability relative to small perturbation of the initial state from the equilibrium. Thus in what follows, by using the Li–Muldowney geometric approach [35], we aim to establish the global and asymptotical stability of the equilibrium P^* for system (1) when $R_0 > 1$.

Theorem 6. *When* $R_0 > 1$, *the worm-existence equilibrium* P^* *is globally asymptotically stable in* $\mathrm{int}(\Omega)$.

Remark 4. The global and asymptotical stability of P^* in $\mathrm{int}(\Omega)$ means that the region $\Omega - \{(V, E, I, Q, S) | I = 0\}$ is a globally asymptotically stable region for the worm-existence equilibrium P^*.

Table 3
The conditions of asymptotical stability (basic reproduction number).

		[16]	[12]	[10]	[19]	This paper
Worm-free	Local	N/A	$R_0 \le 1$	$R_0 \le 1$	$R_0 < 1$	$R_0 \le 1$
Worm-free	Global	$R_0 \le 1$	$R_0 \le 1$	$R_0 \le 1$	$R_0 < 1$	$R_0 \le 1$
Worm-existence	Local	N/A	$R_0 > 1$	$R_0 > 1$	$R_0 > 1$	$R_0 > 1$
Worm-existence	Global	N/A	N/A	$R_0 > 1$	N/A	$R_0 > 1$

Remark 5. The local and global stabilities of the worm-existence equilibrium P^* established in Theorems 5 and 6 tell us that when $R_0 > 1$, all the states $V(t)$, $E(t)$, $I(t)$, $Q(t)$, and $S(t)$ approach to their steady states V^*, E^*, I^*, Q^*, and S^*, respectively, appearing in system (4), as the time t goes to infinity. These results show that $R_0 > 1$ guarantees the network worm is persistent and always spreading within a population, where we can make a prediction of the tendency of the worm propagation in a long run, and assess the level of the popularity of worm attack through the final scale of the infected devices, that is $E^* + I^* + Q^*$.

Note here that the basic reproduction number R_0, as a threshold number, can completely determine the local and global stabilities of the worm-existence equilibrium P^* and govern whether or not the malicious worm is always persistent in time locally and globally among mobile devices.

Finally, we compare the performance of the proposed VEIQS model to those of some existing worm propagation models in terms of asymptotical stability. Refer to Table 3, the stability obtained in our model is similar to those of the existing models.

4. Numerical analysis

In this section, we conduct numerical simulations to analyze the performance and the dynamic behaviors of the VEIQS model, which illustrates the feasibility of the obtained theoretical results.

4.1. Simulation setting

In the real world, it is very difficult to obtain worm traffic traces or realistic parameters. Even in literature (e.g. [36]), some traffic traces are not public. Also, most available traces from CAIDA (www.caida.org) or MIT do not contain the legitimate traffic flow on links since the traces were deliberately filtered before making them available. Then, we are not able to find proper parameters between the worm traffic and the legitimate traffic flow on the same link at the same time. However in this paper, we attempt to determine the parameters from the Slammer worm in next two paragraphs.

Refer to Tables 1 and 2, where the initial parameter values are calculated and chosen carefully to suit a real malicious worm attack scenario. Slammer, one of the fastest-spreading worms, infected 75,000 devices in the first 30 min in January 2003 [1]. Thus, we assume that the total number of devices is $N(0) = 75,000$. Based on the fact that Slammer is a bandwidth-limited worm with an average scan rate $s = 4000$ scans/s [15], the infection rate of the malicious worm can be calculated as $\beta = 0.053$. The natural death rate not due to worm is $\mu = 0.00001$, and the death rate due to worm is $\theta = 0.001$; the state transition rates from E to I, from I to S, and from Q to S, are $\eta = 0.008$, $\gamma = 0.05$, and $\varphi = 0.005$, respectively. The results are based on the average of at least 10 simulation runs [15].

The other parameters in these simulations are given as follows. By the definition of the feasible region Ω, the recruitment rate of all devices is set as $\Lambda = 0.75$. Considering the quarantine control strategy, the quarantine rate of infectious devices is set as $\xi = 0.05$ [18]. The average time for exposed devices to be secured is 1,200 seconds [11], the transition rate from states E to S is $\epsilon = 1/1200 \doteq 0.0008$. To measure the efficiency of the vaccination in a real network environment, the vaccination effective rate is set as $\sigma = 0.6$. Finally, the constant parameter α in the saturated incidence rate is assumed to be 0.8.

4.2. Performance comparison of VEIQS and existing models

To evaluate the performance of the VEIQS model, it is compared by a numerical method with the existing SEIQV [15,16], SEIQR [18], and SEIRS [9] models. All models share the same parameters as those in Section 4.1, and the initial numbers of vulnerable, exposed, infected, quarantined, and secured devices are $V(0) = 74,990$, $E(0) = 0$, $I(0) = 10$, $Q(0) = 0$, and $S(0) = 0$, respectively. In order to measure the impact of the vaccination control strategy, the vaccination coverage rate is set for the vulnerable devices to be $\nu = 0.5$. In Fig. 2, we draw the curves of the numbers of the infectious and secured devices for each of the four models, among which Fig. 2(a) shows that the number of infectious devices and the time it takes to combat the worm in our VEIQS model are both much smaller than those in the other models; Fig. 2(b) shows a noticeable increase and a rapid propagation speed for the secured devices in the VEIQS model than those of the other models. Clearly, the results shown in Fig. 2 validate that the proposed model can more effectively control worm attacks in mobile networks than the other three models.

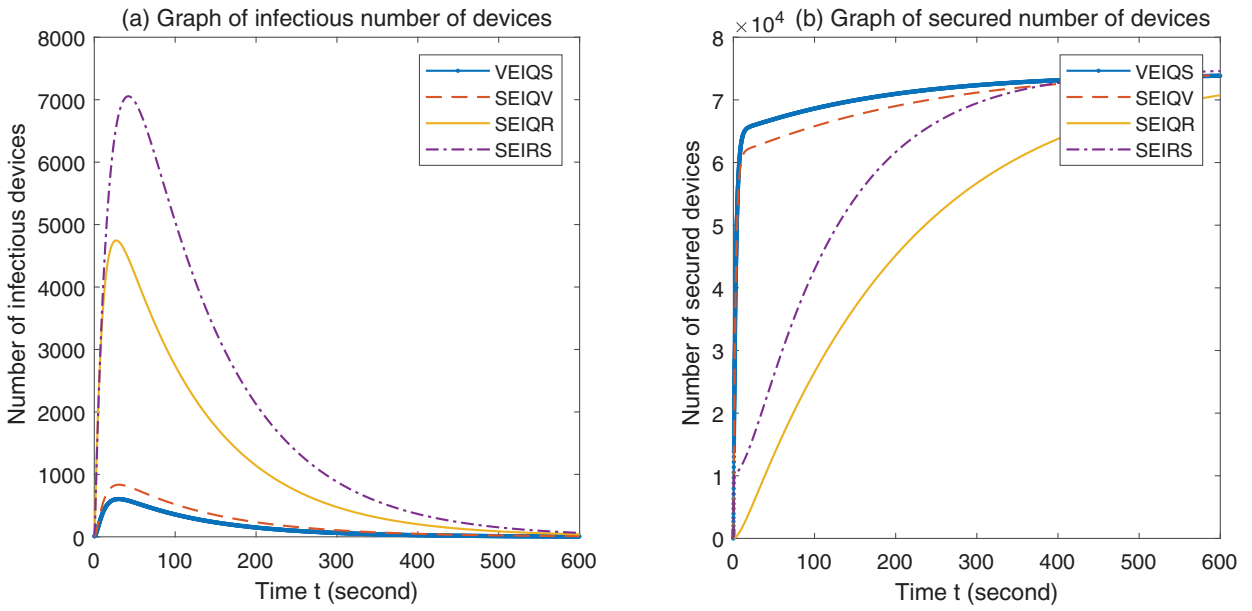

Fig. 2. Performance comparison of VEIQS model to exsiting models.

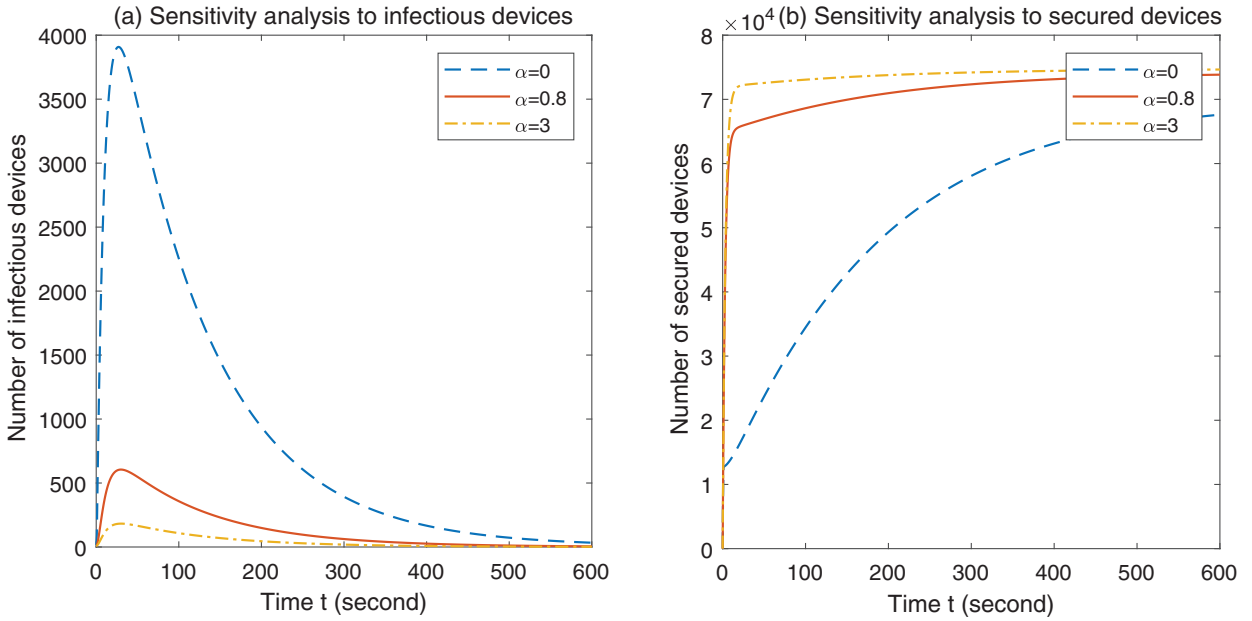

Fig. 3. Sensitivity analysis of parameter α in saturated incidence rate.

4.3. Sensitivity analysis of parameter α in saturated incidence rate

In this subsection, we perform a numerical simulation to analyze the sensitivity of constant parameter α in the saturated incidence rate, where we choose $\alpha = 0,\ 0.8$, and 3, while keeping other parameters of our model the same as those in Section 4.2. See Fig. 3, the effect of the parameter α on the number of infectious devices is depicted in Fig. 3(a), which shows that the larger the parameter α is, the smaller the number of the infectious devices is and the slower the worm spreads at the early stage; the effect of the parameter α on the number of secured devices is depicted in Fig. 3(b), which shows that a larger parameter α can cause a larger number of devices to become secured at a much faster speed. This analysis indicates that by enlarging the parameter α, we can effectively reduce the intensity of worm outbreak.

In particular, when $\alpha = 0$, namely that the proposed VEIQS model is equipped with a bilinear incidence rate, not the saturated incidence rate, it can be seen from Fig. 3 that the worm can propagate more quickly and last much longer in the

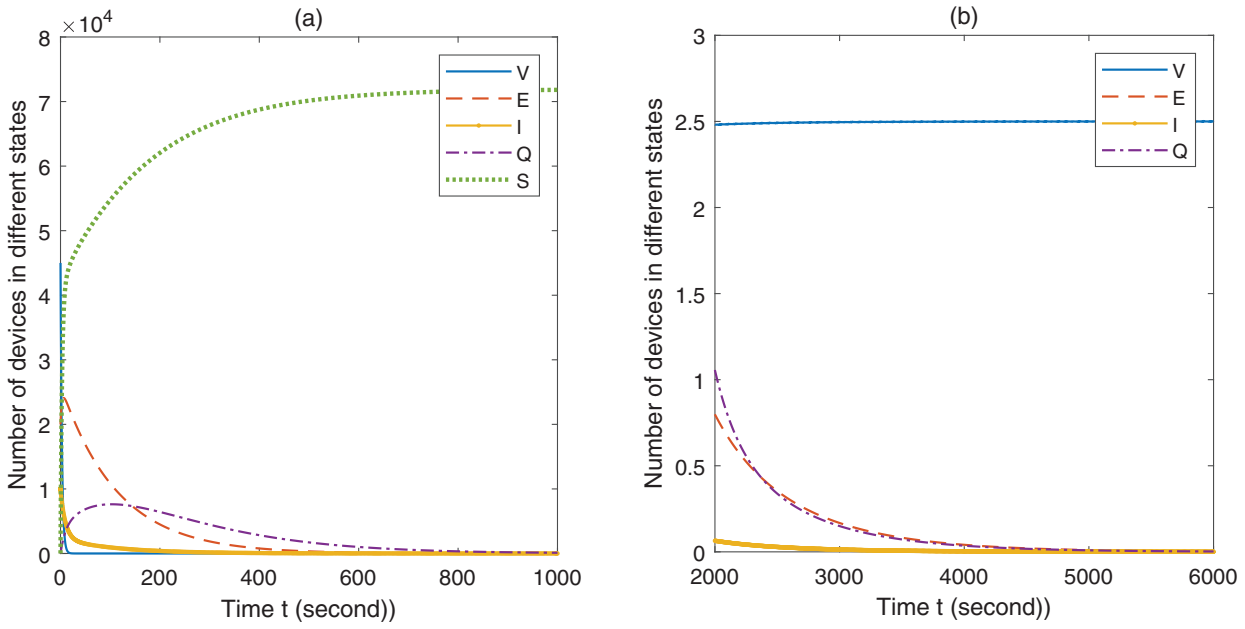

Fig. 4. Dynamics of the worm-free equilibrium.

mobile networks, and the number of infectious devices are much greater; meanwhile, the number of the devices becoming secured from all states is smaller and reaches its maximum in a longer term. The argument tells us that the saturated incidence rate is more reasonable and effective than the bilinear incidence rate to mitigate the worm attack in mobile networks.

4.4. Stabilities of worm-free and worm-existence equilibria

In this subsection, we conduct a numerical experiment for two sets of parameters that illustrate the dynamic behavior of the VEIQS model depending on the value of the basic reproduction number.

Firstly, the initial numbers of modelling states are set as $V(0) = 45,000,\ E(0) = 20,000,\ I(0) = 10,000,\ Q(0) = 0,$ and $S(0) = 0,$ and the parameters are set as the same as those in Section 4.2. By using Eq. (2), the worm-free equilibrium $P_0 = (2.5, 0, 0, 0, 74997.5),$ and by Eq. (3), the basic reproduction number $R_0 = 0.8338 < 1$. Thus by Theorems 2 and 3, the worm-free equilibrium (2.5, 0, 0, 0, 74997.5) is locally and globally asymptotically stable, which means that as the time t goes to infinity, $V(t)$ and $S(t)$ approach to their steady states 2.5 and 74997.5, but $E(t)$, $I(t)$, and $E(t)$ approach to 0. Especially, the final scale of the infected devices, namely, $E_0 + I_0 + Q_0$, is equal to 0, which suggests that the worm is dying out, the infected devices will gradually disappear, and the worm attack is under control eventually. From Fig. 4, we observe that the tendency of the worm propagation is depressive in a long run, and the final size of infected devices is gradually vanishing in the end, which is consistent with the theoretic results as those in Theorems 2 and 3.

Secondly, we set the vaccination coverage rate as $\nu = 0.1,$ and the initial numbers of modelling states and the other parameters as those in Section 4.2. Based on these numerical values, we obtain, by Eq. (4), that the unique worm-existence equilibrium $P^* = (7.27, 35.61, 2.82, 23.46, 72298.8),$ and by Eq. (3), the basic reproduction number $R_0 = 5.597 > 1$. Hence by Theorems 5 and 6, the worm-existence equilibrium (7.27, 35.61, 2.82, 23.46, 72298.8) is locally and globally asymptotically stable, which shows that as the time t goes to infinity, $V(t)$, $E(t)$, $I(t)$, $Q(t)$, and $S(t)$ all approach to their steady states 7.27, 35.61, 2.82, 23.46, and 72298.8, respectively. The local and global stability of worm-existence equilibrium gives a prediction of the tendency of the worm propagation among mobile devices, see Fig. 5. From this analysis, the final scale of the infected devices, $E^* + I^* + Q^*,$ is derived as 61.89, and the worm is always spreading in a population 61.89, which can be used to assess the level of the popularity of worm attacks in mobile networks. The numerical simulation results are shown in Fig. 5, in which Fig. 5(a) gives roughly the curves of $V(t)$, $E(t)$, $I(t)$, $Q(t)$, and $S(t)$ in a short period; Fig. 5(b) presents further details of $V(t)$, $E(t)$, $I(t)$, and $Q(t)$, and plots the tendency of the worm propagation in a later period, which are consistent with the theoretic results in Theorems 5 and 6.

Besides, for the global stability, we incorporate two 3-dimensional figures by considering different initial numbers of modelling states, namely, $(V(0), E(0), I(0), Q(0), S(0)) = (74, 990, 0, 10, 0, 0),\ (68, 000, 2000, 5000, 0, 0),$ or $(59, 000, 6000, 10, 000, 0, 0)$. The model parameters are the same as those in the above second case for the global stability. See Fig. 6(a) and (b), we see that the system (1) ultimately reaches the worm-existence equilibrium point. Precisely, Fig. 6(a) indicates that for different initial values, $(V(t), E(t), S(t))$ ultimately converges to the point (V^*, E^*, S^*); while in Fig. 6(b), $(I(t),$

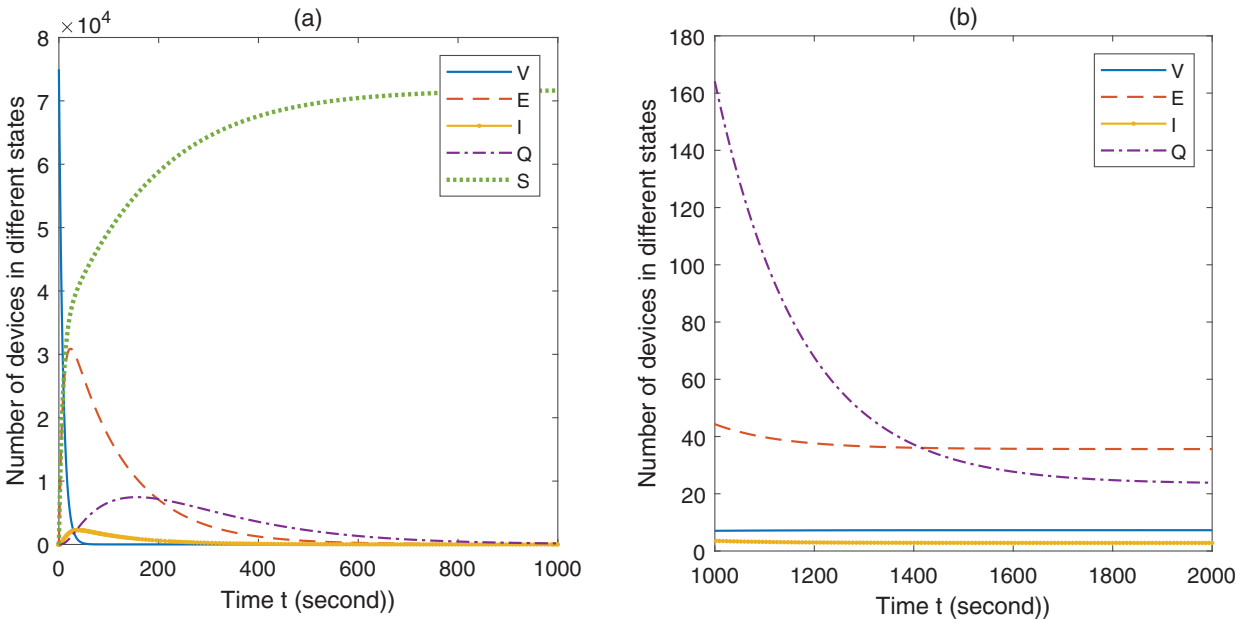

Fig. 5. Dynamics of the worm-existence equilibrium.

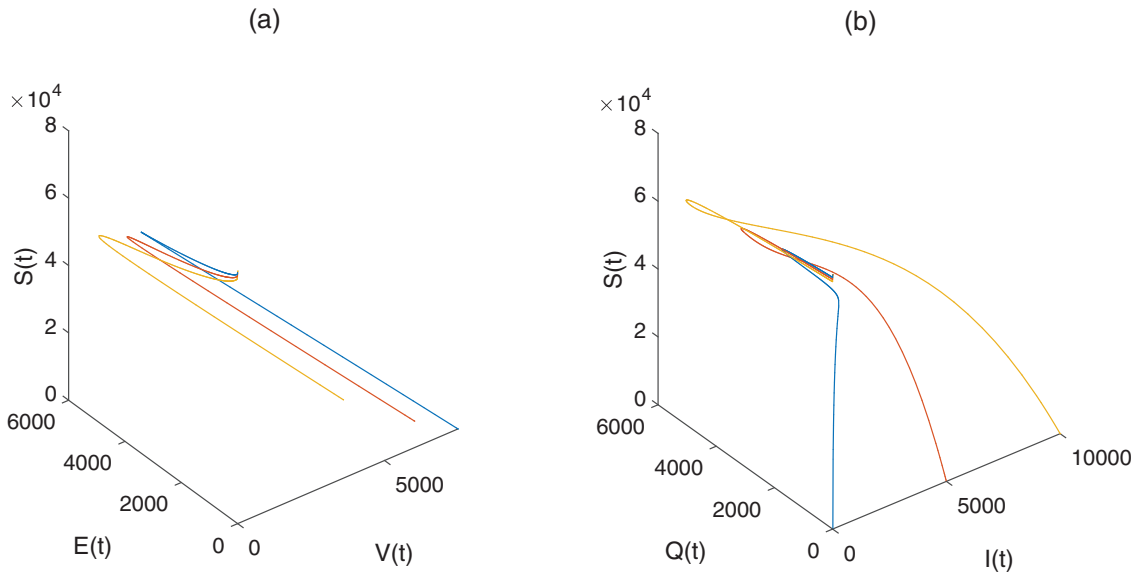

Fig. 6. Global dynamics with different initial numbers of modelling states.

$Q(t)$, $S(t)$) converges to the point (I^*, Q^*, S^*). Consequently, Fig. 6 can enable us to evaluate the unique worm-existence equilibrium numerically.

As shown in Figs. 4–6, the infected devices (including exposed, infectious, and quarantined devices) will gradually disappear or tend to a minuscule scale, and almost all devices in the system become secured after a period of time. This illustrates that the worm attack does exist but be of small size, which is mainly thanks to the control strategies of vaccination, quarantine and others adopted in the proposed VEIQS model. The simulation results show the feasibility and rationality of our VEIQS model with control strategies.

5. Control strategies

It is well-known that "optimal control strategy" or "impulse control strategy" is commonly used by mathematical approaches to control some disease, see [37–39], and the corresponding region plot, an improved numerical simulation, can

be found in literature [37,40,41]. Also, for discrete-time systems, a new output feedback H_∞ control method is mentioned in [42,43]. So in this paper, we firstly present the optimal control strategy based on Pontryagin's Minimum Principle [44], and secondly from the explicit expression (3) of the basic reproduction number R_0, we give some control strategies to prevent the worm propagation through mobile networks. Besides, we carry out the corresponding numerical simulations to illustrate the effectiveness of these obtained control strategies.

5.1. The optimal control strategy (or impulse control)

In this subsection, we construct an optimal control strategy to minimize the systemic cost of vaccination and quarantine as well as minimize the infected mobile devices (including exposed and infectious ones) and maximize the secured devices. So in the VEIQS model described by (1), we choose two control variables $u_1(t)$ and $u_2(t)$, which, respectively, represent the inhibiting effect on worm infection in mobile networks by the vaccination and quarantine strategies satisfying $0 \le u_i(t) \le 1$, $i = 1, 2$. In particular, $u_1(t) = 1$ (or $u_2(t) = 1$) means the maximal use of vaccination (or quarantine), and $u_1(t) = 0$ (or $u_2(t) = 0$) means no vaccination (or quarantine). The optimal control problem is formulated as

$$J(u_1, u_2) = \int_{t_0}^{t_f} [Ku_1^2(t) + Lu_2^2(t) + E(t) + I(t) - S(t)]dt,$$

subject to the state system

$$\begin{cases} V'(t) = \Lambda - \dfrac{(1-u_1(t))\beta VI}{1+\alpha I} - (u_1(t)+\mu)V, \\ E'(t) = \dfrac{(1-u_1(t))\beta VI}{1+\alpha I} - (\eta+\epsilon+\mu)E, \\ I'(t) = \eta E - (u_2(t)+\gamma+\mu+\theta)I, \\ Q'(t) = u_2(t)I - (\varphi+\mu+\theta)Q, \\ S'(t) = u_1(t)V + \epsilon E + \gamma I + \varphi Q - \mu S, \end{cases} \tag{5}$$

where the parameters $K \ge 0$ and $L \ge 0$ are the weights on the benefits of the cost of vaccination and quarantine, respectively. Our main goal is to seek the optimal control pair (u_1^*, u_2^*) such that

$$J(u_1^*, u_2^*) = \min\{J(u_1, u_2) : (u_1, u_2) \in U\}, \tag{6}$$

where U is the control set defined by $U = U_1 \times U_2 = \{(u_1(t), u_2(t)) : u_1(t)$ and $u_2(t)$ are measurable, $0 \le u_1(t) \le 1, 0 \le u_2(t) \le 1, t \in [t_0, t_f]\}$.

In order to determine the optimal control pair (u_1^*, u_2^*), we first discuss its existence by Fleming and Rishel [45].

Theorem 7. *There exists an optimal control pair $(u_1^*, u_2^*) \in U$ such that (6) subject to the state system (5) with the initial conditions at time t_0.*

For the state system (5), we derive the Hamiltonian as follows:

$$\begin{aligned} H = {} & Ku_1^2 + Lu_2^2 + E + I - S + w_1\left[\Lambda - \frac{(1-u_1)\beta VI}{1+\alpha I} - (u_1+\mu)V\right] + w_2\left[\frac{(1-u_1)\beta VI}{1+\alpha I} - (\eta+\epsilon+\mu)E\right] \\ & + w_3[\eta E - (u_2+\gamma+\mu+\theta)I] + w_4[u_2 I - (\varphi+\mu+\theta)Q] + w_5[u_1 V + \epsilon E + \gamma I + \varphi Q - \mu S]. \end{aligned} \tag{7}$$

Then by applying the Pontryagin's Minimum Principle [44] to the Hamiltonian (7), we obtain the following theorem.

Theorem 8. *Given an optimal control pair (u_1, u_2) and corresponding solution of the state system (5), there exist adjoint variables w_i, $i = 1, \ldots, 5$, satisfying the adjoint system of equations as*

$$\begin{cases} w_1'(t) = -\dfrac{\partial H}{\partial V} = \dfrac{(w_1-w_2)(1-u_1)\beta I}{1+\alpha I} + (w_1-w_5)u_1 + w_1\mu, \\ w_2'(t) = -\dfrac{\partial H}{\partial E} = -1 + (w_2-w_3)\eta + (w_2-w_5)\epsilon + w_2\mu, \\ w_3'(t) = -\dfrac{\partial H}{\partial I} = -1 + \dfrac{(w_1-w_2)(1-u_1)\beta V}{(1+\alpha I)^2} + (w_3-w_4)u_2 + (w_3-w_5)\gamma + w_3(\mu+\theta), \\ w_4'(t) = -\dfrac{\partial H}{\partial Q} = (w_4-w_5)\varphi + w_4(\mu+\theta), \\ w_5'(t) = -\dfrac{\partial H}{\partial S} = 1 + w_5\mu, \end{cases} \tag{8}$$

with boundary conditions $w_i(t_f) = 0$, for $i = 1, \ldots, 5$. Furthermore, the optimal control pair (u_1^*, u_2^*) for (5) such that (6) is characterized by

$$\begin{cases} u_1^* = \max\left\{0, \min\left\{1, \dfrac{1}{2K}\left[\dfrac{(w_2 - w_1)\beta VI}{1+\alpha I} + (w_1 - w_5)V\right]\right\}\right\}, \\ u_2^* = \max\left\{0, \min\left\{1, \dfrac{(w_3 - w_4)I}{2L}\right\}\right\}. \end{cases} \tag{9}$$

Remark 6. The optimality system consists of the state system (5), the adjoint system (8) with the initial and boundary conditions, and the optimal control pair (u_1^*, u_2^*) characterized by (9), which means that the optimality system is shown as

$$\begin{cases} V'(t) = \Lambda - \dfrac{(1-u_1^*)\beta VI}{1+\alpha I} - (u_1^* + \mu)V, \\ E'(t) = \dfrac{(1-u_1^*)\beta VI}{1+\alpha I} - (\eta + \epsilon + \mu)E, \\ I'(t) = \eta E - (u_2^* + \gamma + \mu + \theta)I, \\ Q'(t) = u_2^* I - (\varphi + \mu + \theta)Q, \\ S'(t) = u_1^* V + \epsilon E + \gamma I + \varphi Q - \mu S, \\ w_1'(t) = -\dfrac{\partial H}{\partial V} = \dfrac{(w_1 - w_2)(1-u_1^*)\beta I}{1+\alpha I} + (w_1 - w_5)u_1^* + w_1\mu, \\ w_2'(t) = -\dfrac{\partial H}{\partial E} = -1 + (w_2 - w_3)\eta + (w_2 - w_5)\epsilon + w_2\mu, \\ w_3'(t) = -\dfrac{\partial H}{\partial I} = -1 + \dfrac{(w_1 - w_2)(1-u_1^*)\beta V}{(1+\alpha I)^2} + (w_3 - w_4)u_2^* + (w_3 - w_5)\gamma + w_3(\mu + \theta), \\ w_4'(t) = -\dfrac{\partial H}{\partial Q} = (w_4 - w_5)\varphi + w_4(\mu + \theta), \\ w_5'(t) = -\dfrac{\partial H}{\partial S} = 1 + w_5\mu, \end{cases}$$

with boundary conditions, $w_i(t_f) = 0$, for $i = 1, \ldots, 5$, and initial conditions at time t_0.

For the proofs of Theorems 7 and 8, the readers are referred to Appendixes A.7 and A8. Using Lemma 4.1 of Joshi [46] and following the proof of Theorem 2 of [39], the uniqueness of the optimality system is obtained immediately.

Theorem 9. *The solution of the optimality system is unique for sufficient small t_f.*

Finally, we conduct some numerical simulations to illustrate the effectiveness of the optimal control theoretic approach. The initial numbers and the parameters of model (1) are taken as the same as those in Section 4.2. As shown in Fig. 7, we give the system dynamics with control and without control, of which more details are presented as follows:

1. Fig. 7(a) depicts the trend of the number of vulnerable devices over time with control and without control. It is seen that in absence of control, the number of vulnerable devices is negligible all the time, which means that almost all the vulnerable ones will be infected immediately by the malicious worms once they are caught in the mobile networks.
2. Fig. 7(b) depicts the trend of the number of exposed devices over time with control and without control, where we observe that the number of exposed devices with control is much smaller than that without control, and also in presence of the optimal control, the exposed devices last shorter in mobile environment.
3. Fig. 7(c) depicts the trend of the number of infectious devices over time with control and without control, where we find that without control, the maximum number of infectious devices is nearly 8000, while with control, the maximum number of infectious ones is much smaller, namely 600, and the worm will disappear soon once it breaks out.
   From Fig. 7(b) and (c), we conclude that by using the optimal control, the worm lasts much shorter in mobile networks, and the mobile devices infected by this worm (including exposed and infectious ones) becomes fewer.
4. Fig. 7(d) depicts the trend of the number of secured devices over time with control and without control, which indicates that the number of secured devices with control is larger and reaches its maximum much faster than that without control. So in presence of control, a larger number of mobile devices become secured at much faster speed.

In conclusion, the numerical results of Fig. 7 demonstrates that by introducing an optimal control into a system can have a profound effect on mobile devices, and the optimal control techniques provide effective tools to defend against worm attacks.

5.2. Control strategies based on R_0

As was stated in Section 3 and 4.4, the basic reproduction number R_0 is a sharp threshold value completely determining the dynamic behaviors of the VEIQS model in the feasible region. Besides, this threshold value plays a critical role to control

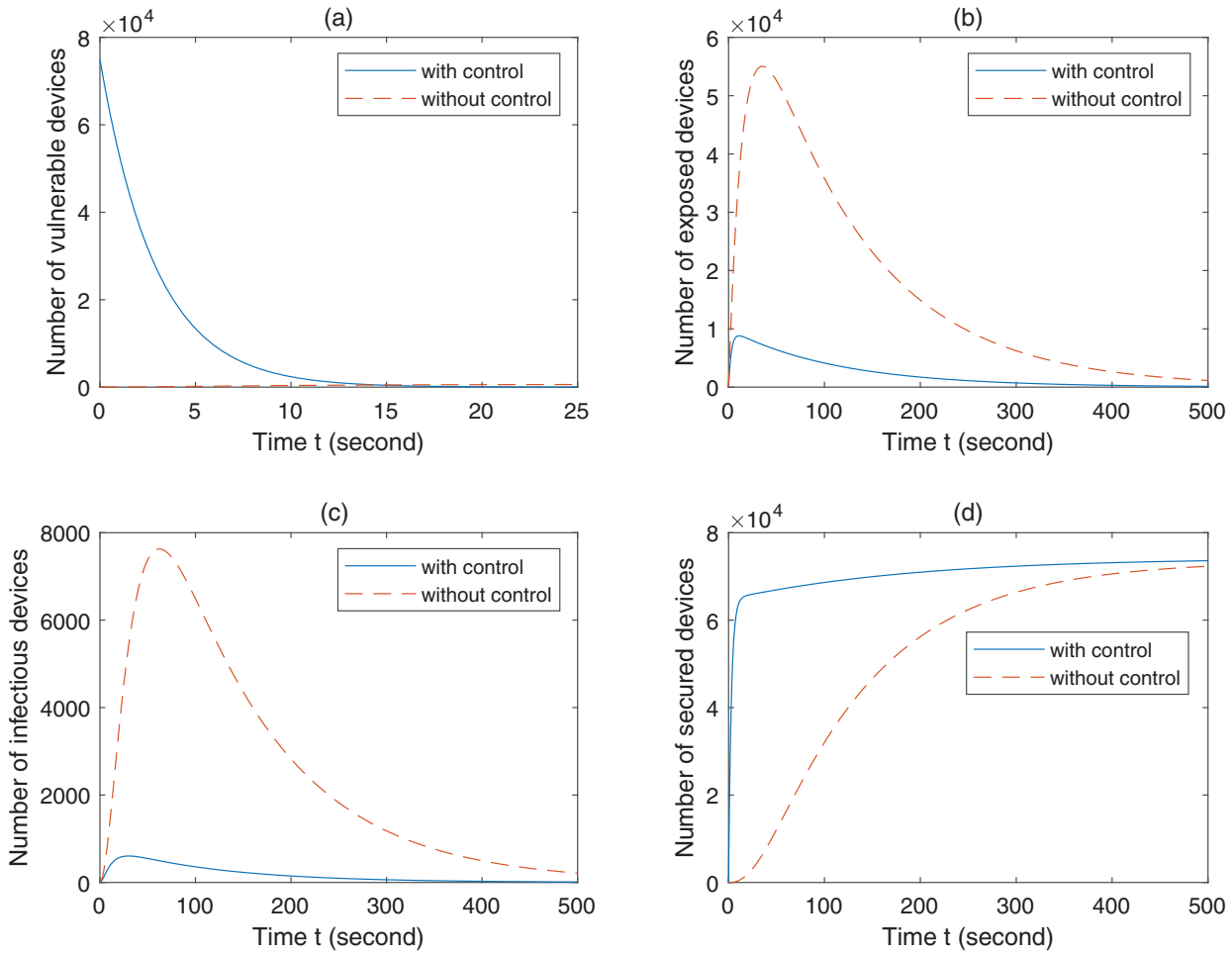

Fig. 7. System dynamics with control and without control.

an epidemic of worm among mobile devices. In fact, by Theorems 2 and 3, we obtain the local and global stabilities of the worm-free equilibrium P_0 under the condition that $R_0 \leq 1$. Thus, in order to prevent a mobile-network based worm outbreak from becoming an epidemic and then mitigate the intensity of the epidemic, we control the corresponding parameters to make $R_0 \leq 1$. From Eq. (3), the basic reproduction number R_0 depends on the parameters as follows: the recovery coefficients ϵ and γ, the infection rates β and η from states V and E, the natural and worm-related death rates μ and θ, the quarantine rate ξ, vaccination effective and coverage rates σ and ν, and recruitment rate Λ. Note that the threshold parameter does not depend on the recovery rate φ from states Q to S.

Based on Theorems 2 and 3, we have a statement below regarding the parameters in (3), in order to prevent the widespread of worms and decrease its attack through mobile networks. We delay its proof to Appendix A9.

Corollary 1. *To stop the worm attack in mobile networks, the parameters should satisfy the following conditions:*

$$\Lambda < \frac{(\sigma\nu+\mu)(\xi+\gamma+\theta+\mu)}{(1-\sigma\nu)\beta};\ \beta < \frac{(\sigma\nu+\mu)(\xi+\gamma+\theta+\mu)}{(1-\sigma\nu)\Lambda};\ \sigma\nu > \frac{\beta\Lambda-\mu(\xi+\gamma+\theta+\mu)}{\xi+\gamma+\theta+\mu+\beta\Lambda};$$

$$\gamma > \frac{(1-\sigma\nu)\beta\Lambda}{\sigma\nu+\mu} - (\xi+\theta+\mu);\ \xi > \frac{(1-\sigma\nu)\beta\Lambda}{\sigma\nu+\mu} - (\gamma+\theta+\mu);\ \theta > \frac{(1-\sigma\nu)\beta\Lambda}{\sigma\nu+\mu} - (\xi+\gamma+\mu);$$

$$\epsilon > \frac{(1-\sigma\nu)\beta\eta\Lambda}{(\sigma\nu+\mu)(\xi+\gamma+\theta+\mu)} - (\eta+\mu);$$

and

$$\eta < \frac{(\sigma\nu+\mu)(\epsilon+\mu)(\xi+\gamma+\theta+\mu)}{(1-\sigma\nu)\beta\Lambda-(\sigma\nu+\mu)(\xi+\gamma+\theta+\mu)},\quad if\quad (1-\sigma\nu)\beta\Lambda > (\sigma\nu+\mu)(\xi+\gamma+\theta+\mu);$$

or

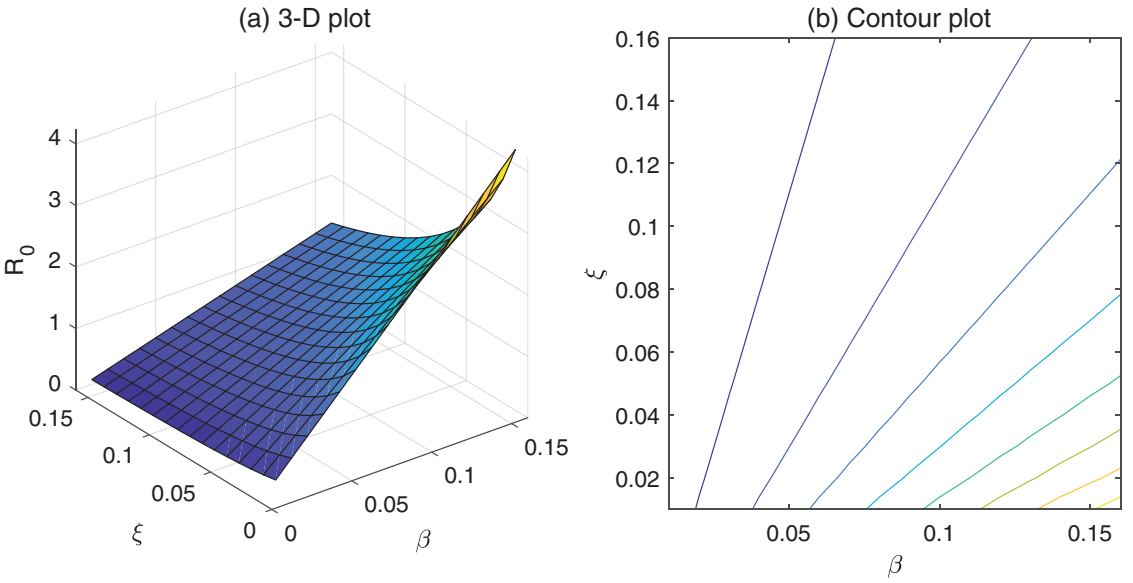

Fig. 8. Analysis of R_0.

$$\eta > \frac{(\sigma\nu+\mu)(\epsilon+\mu)(\xi+\gamma+\theta+\mu)}{(1-\sigma\nu)\beta\Lambda-(\sigma\nu+\mu)(\xi+\gamma+\theta+\mu)}, \quad if \quad (1-\sigma\nu)\beta\Lambda < (\sigma\nu+\mu)(\xi+\gamma+\theta+\mu).$$

Taking into account the numeric values for the parameters as the same as those in Section 4.2 except σ and ν, we conclude that the transition from the worm-free regimen to the worm-existence regimen occurs when $\sigma\nu = 0.1787$, which matches well with the lower-bound of $\sigma\nu$ appearing in Corollary 1. The same concerns the other parameters.

Taking partial derivatives of R_0 in Eq. (3), we have

$$\frac{\partial R_0}{\partial\sigma} < 0, \quad \frac{\partial R_0}{\partial\nu} < 0, \quad \frac{\partial R_0}{\partial\beta} > 0, \quad \frac{\partial R_0}{\partial\eta} > 0, \quad \frac{\partial R_0}{\partial\Lambda} > 0, \quad \frac{\partial R_0}{\partial\mu} < 0, \quad \frac{\partial R_0}{\partial\epsilon} < 0,$$
$$\frac{\partial R_0}{\partial\xi} < 0, \quad \frac{\partial R_0}{\partial\gamma} < 0, \quad \text{and} \quad \frac{\partial R_0}{\partial\theta} < 0,$$

which show that if we set all variables of R_0 constant except only one, the function R_0 decreases as the parameters β, η, and Λ decrease or the parameters σ, ν, μ, ϵ, ξ, γ, and θ increase. Thus, to reduce the value of R_0, we could reduce the numeric values of β, η, and Λ, or increase the values of σ, ν, μ, ϵ, ξ, γ, and θ. See, for example, the 3-dimensional plot and Contour plot in Fig. 8, which further describes the trend of R_0 over time with different transmission rates β and ξ. It can be seen that R_0 increases in β and decreases in ξ. The same concerns the other transmission rates.

From the above analysis of the basic reproduction number, the following control measures are obtained to prevent the worm propagation through mobile networks and then control the worm outbreak among mobile devices. Meanwhile, the corresponding numerical simulations are carried out to illustrate the effectiveness of the obtained measures, especially the impacts of the given parameters on the number of infectious devices and the speed of worm propagation. Notice here that the infectious number and the propagation speed are two key factors in determining the intensity of worm attack.

1. Reducing the infection rate β of vulnerable devices by installing efficient antivirus softwares or immunization procedures. A numerical experiment of this strategy is conducted to evaluate the impact on the infectious devices with different infection rates $\beta = 0.1$, 0.053, and 0.01. The initial numbers of modelling states and the other parameters are set as the same as those in Section 4.2. From Fig. 9(a), we see that as the infection rate β decreases, the number of infectious devices and the time taken to combat the worm become much smaller.
2. Reducing the infectious rate η from the exposed state. In order to investigate the impact of this infectious rate on the infectious devices, we set the different values for η as 0.008, 0.003, and 0.001, and set the initial numbers of modelling states and the other parameters as those in Section 4.2. As shown in Fig. 9(b), the smaller the infectious rate η is, the fewer vulnerable devices are infected in a long run, which indicates that the worm propagates more slowly with the reduction of infectious rate.
3. Increasing the quarantine rate ξ by enhancing the quarantine capabilities. In the following numerical experiment, we consider the effect of changing the quarantine rate on the worm propagation. Set $\xi = 0.03$, 0.05, and 0.09, and the initial numbers of modelling states and the other modelling parameters are the same as those in Section 4.2. See Fig. 9(c), a higher quarantine rate results in lowering the number of infectious devices, diminishing the worm

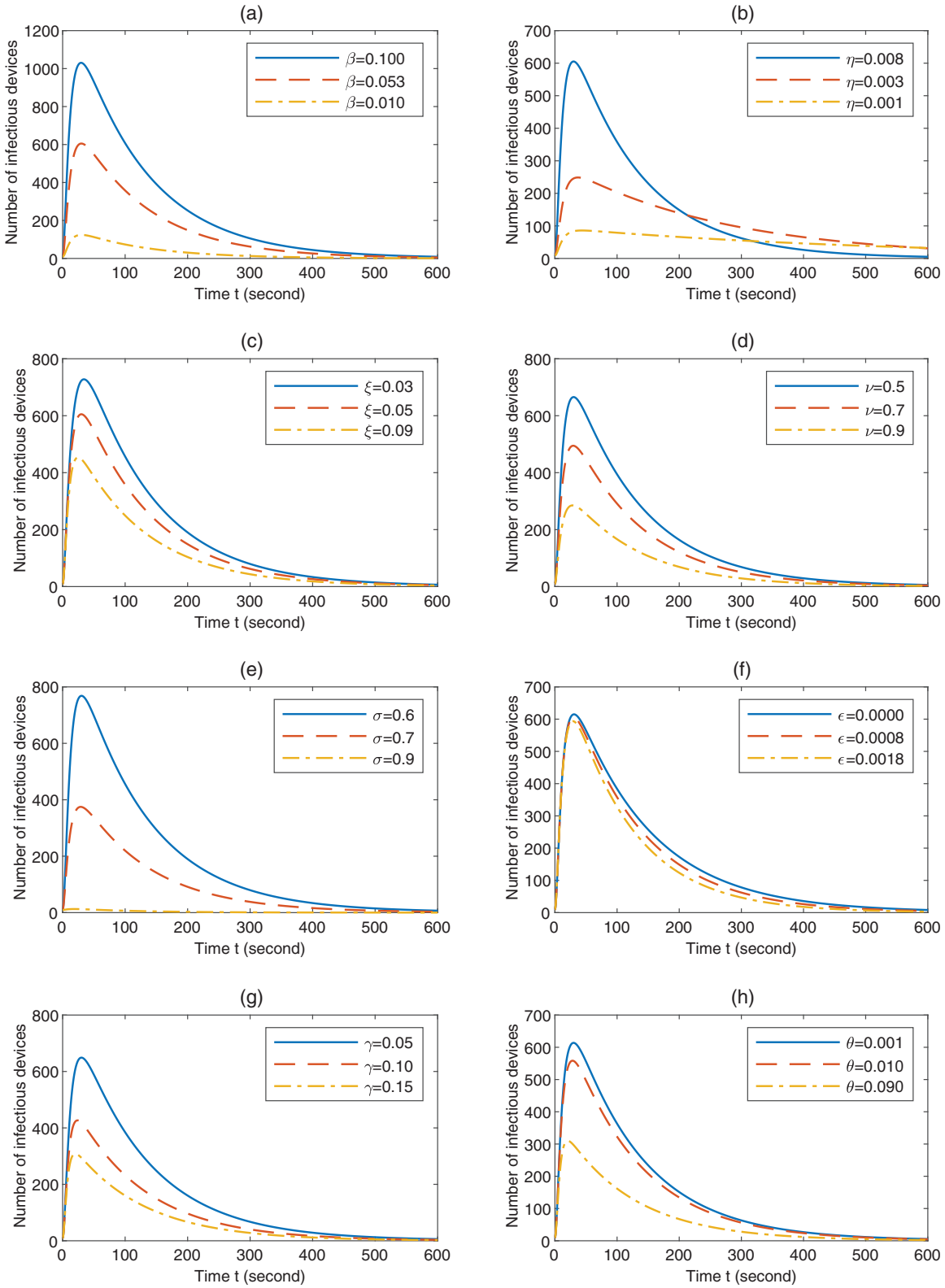

Fig. 9. Impacts of the modelling parameters on the infectious devices.

propagation speed, and shortening the time taken to combat the worm. Clearly, the quarantine strategy is pretty effective to mitigate the worm attack, which is because the higher quarantine rate causes fewer infectious devices able to infect other devices, so that fewer devices can be infected at every time.

4. Increasing the vaccination coverage rate ν by enlarging the user scale of antivirus software. Conduct a numerical experiment to show the impact of the vaccination coverage rate on the infectious devices with different values $\nu = 0.5,\ 0.7$, and 0.9, where the initial numbers of modelling states and the other parameters are the same as those in Section 4.2. From the curves plotted in Fig. 9(d), we observe that with the increase of the vaccination coverage rate, the total number of infectious devices become smaller, the worm propagation speed become lower, and the time taken to combat the worm propagation is shorter.
5. Increasing the vaccination effective rate σ of antivirus software by improving the quality of antivirus software. Set $\sigma = 0.6,\ 0.7$, and 0.9, and the initial numbers of modelling states and the other parameters as those in Section 4.2. The impact of the vaccination efficiency on the infectious devices is shown in Fig. 9(e), in which when $\sigma = 0.6$, the maximum number of infectious devices is nearly 800; when $\sigma = 0.9$, the number of infectious devices is negligible, and the worm will die out soon after it breaks out. Then, improving the vaccination efficiency of antivirus software can reduce the number of infectious devices and the time it takes to combat the worm propagation in mobile networks.
6. Increasing the recovery rate ϵ from the exposed state by sensitizing users to install security countermeasures. In this experiment, we consider the effect of the recovery rate on the infectious devices with different values $\epsilon = 0,\ 0.0008$, and 0.0018. The initial numbers of modelling states and the other parameters are the same as those in Section 4.2. From Fig. 9(f), it can be seen that the larger the recovery rate is, the fewer devices are infected in a shorter time, which shows that the worm propagates more slowly in the mobile networks with the increase of recovery rate ϵ.
7. Increasing the recovery rate γ from the infectious state by improving the performance of antivirus software. Now we vary the recovery rate γ to study its impact on the infectious devices, where $\gamma = 0.05,\ 0.10$, and 0.15, and the initial numbers of modelling states and the other parameters are the same as those in Section 4.2. Fig. 9(g) illustrates that the worm propagates in a shorter term and infects fewer devices in mobile networks as the recovery rate γ increases, which can decrease the intensity of worm attack since a larger recovery rate γ can reduce the number of the infectious devices that are able to infect other devices; so that fewer devices can be infected at every time.
8. Increasing the death rate θ that is related to worm. Set three values for $\theta = 0.001, 0.01$, and 0.09, to analyze their impact on the infectious devices, where the initial numbers of modelling states and the other parameters are set as those in Section 4.2. The curves in Fig. 9(h) show that as the worm-related death rate increases, the worm propagates more slowly and lasts much shorter in mobile networks, and the mobile devices infected by this worm becomes fewer.

Theoretically, increasing the natural death rate μ can reduce the basic reproduction number and thus control the worm breakout. By a simple calculation, the elasticity of the basic reproduction number R_0 with respect to μ is

$$E_\mu = \frac{\partial R_0}{\partial \mu} \cdot \frac{\mu}{R_0} = -\mu\left(\frac{1}{\sigma\nu + \mu} + \frac{1}{\eta + \epsilon + \mu} + \frac{1}{\xi + \gamma + \theta + \mu}\right).$$

Considering the parameters as the same as those in Section 4.2, we have $E_{\mu=0.00001} = 0.001$, which means that as the natural birth rate increases 1% at $\mu = 0.00001$, the basic reproductive number R_0 only decreases 0.001% correspondingly. From this, we conclude that the worm propagation is less sensitive to the natural death rate μ. Hence, the control strategy by increasing the natural death rate μ is not effective and feasible strategies to defend against the attack of worms.

6. Conclusions and future research direction

In this paper, we propose a new VEIQS model for worm propagation with a saturated incidence rate in mobile networks, where the saturated incidence rate is more reasonable and effective than a bilinear incidence rate, since it considers the crowding effect of the infectious devices and prevents the unboundedness of the contact rate by choosing suitable parameters. Besides, the novel idea in the proposed model is to combine the control strategies of vaccination, quarantine and others for preventing, detecting, and defending against the intensity of an outbreak of worm through mobile networks.

The basic reproduction number R_0 is obtained to completely determine the global and local stabilities of worm propagation and how intensive a policy will need to be to control the worm attack. Our results show that when $R_0 \leq 1$, the worm-free equilibrium is locally and globally asymptotically stable, implying that the worm is dying out, the infected devices will gradually disappear, and the worm attack remains under control eventually; when $R_0 > 1$, by using the Li–Muldowney geometric approach, the unique worm-existence equilibrium is locally and globally asymptotically stable, namely that the worm is always persistent and spreading within a population. This paper provides some novel insights to cyber security, including establishing the control strategies to fight against worm attack, predicting the tendency of worm propagation and measuring the level of the worm popularity by the final scale of the infected devices. Numerical simulations are also implemented to illustrate the feasibility of the theoretical results.

Based on Pontryagin's Minimum Principle [44], we present an optimal control strategy to minimize the systemic cost of vaccination and quarantine as well as minimize the infected mobile devices (including exposed and infectious ones)

and maximize the secured devices. Also, by the explicit expression of the basic reproduction number, we give the efficient worm-epidemic control strategies to prevent the worm propagation through mobile networks and then mitigate the risk of the worm outbreak among mobile devices, including the reduction of the infection rates from vulnerable and exposed sates, and the increase of the quarantine rate, vaccination effective and coverage rates, worm-related death rate, and the recovery rates from exposed and infectious states. And by enlarging the parameter in the saturated incidence rate, we can control the worm attack. Meanwhile, the corresponding numerical simulations are carried out to illustrate the effectiveness of the obtained strategies.

The numerical values of the model parameters used in this paper are collected from different existing papers, see Section 4.1. However in the real world, most available traces from CAIDA (www.caida.org) or MIT do not contain the legitimate traffic flow on links since the traces were deliberately filtered before making them available, we have to say that it is very hard to use some real-world worm traffic traces or realistic parameters for research. In the further work, we will consider the dynamic quarantine strategy employed simultaneously in the vulnerable, exposed, and infectious states, not only in the infectious state. The quarantine time and the delay of the mobile networks may be taken into consideration.

Acknowledgments

The authors would like to thank the four anonymous referees for their valuable comments which can improve the presentation and the quality of the earlier version of this paper. The first author is supported by the National Natural Science Foundation of China (Nos. 11501295 and 11871289), the Postdoctoral Science Foundation of China (No. 2015M580415), the Natural Science Foundation of Jiangsu Province of China (No. BK20151459), the Social Science Foundation of Jiangsu Province of China (No. 16GLC006), the Postdoctoral Science Foundation of Jiangsu Province of China (No. 1501004B) and Qing-Lan Project of Jiangsu Province. The second author is partially supported by the United States National Science Foundation (NSF) under award number 1762807. However, any opinions, findings, and conclusions or recommendations in this document are those of the authors and do not necessarily reflect views of the NSF.

Appendix A. Proofs of theorems and corollary

A1. Proof of Theorem 1. The equilibrium points are the solutions of the following system:

$$\begin{cases} V'(t) = 0, \\ E'(t) = 0, \\ I'(t) = 0, \\ Q'(t) = 0, \\ S'(t) = 0. \end{cases}$$

From $I'(t) = 0$, we have

$$E = \frac{\xi + \gamma + \mu + \theta}{\eta} I.$$

Substituting this into $E'(t) = 0$ leads to

$$\left[\frac{(1 - \sigma\nu)\beta V}{1 + \alpha I} - \frac{(\eta + \epsilon + \mu)(\xi + \gamma + \mu + \theta)}{\eta} \right] I = 0.$$

Then, the equilibrium occurs at:

$$I = 0, \quad \text{or} \quad I > 0 \ \text{ and } \ V = \frac{(\eta + \epsilon + \mu)(\xi + \gamma + \mu + \theta)(1 + \alpha I)}{(1 - \sigma\nu)\beta\eta}. \tag{A.10}$$

For $I = 0$, it is easy to see that system (1) always has a unique worm-free equilibrium point of the form (2). For $I > 0$, we substitute the expression of V in (A.10) into $V'(t) = 0$ to get

$$(\eta + \epsilon + \mu)(\xi + \gamma + \mu + \theta)[(1 - \sigma\nu)\beta + \alpha(\sigma\nu + \mu)]I + (\sigma\nu + \mu)(\eta + \epsilon + \mu)(\xi + \gamma + \mu + \theta) - (1 - \sigma\nu)\beta\eta\Lambda = 0.$$

Recalling the expression (3) of the basic reproduction number R_0, we derive that, if $R_0 \le 1$, there is no positive equilibrium, and the worm-free equilibrium is the only equilibrium in Ω; if $R_0 > 1$, there exists a unique positive equilibrium $P^* = (V^*, E^*, I^*, Q^*, S^*)$, called worm-existence equilibrium, in int(Ω), where

$$I^* = \frac{(1 - \sigma\nu)\beta\eta\Lambda - (\sigma\nu + \mu)(\eta + \epsilon + \mu)(\xi + \gamma + \mu + \theta)}{(\eta + \epsilon + \mu)(\xi + \gamma + \mu + \theta)[(1 - \sigma\nu)\beta + \alpha(\sigma\nu + \mu)]},$$

and then V^*, E^*, Q^*, S^* satisfy

$$\begin{cases} V^* = \dfrac{(\eta+\epsilon+\mu)(\xi+\gamma+\mu+\theta)(1+\alpha I^*)}{(1-\sigma\nu)\beta\eta}, \\ E^* = \dfrac{\xi+\gamma+\mu+\theta}{\eta} I^*, \\ Q^* = \dfrac{\xi}{\varphi+\mu+\theta} I^*, \\ S^* = \dfrac{\sigma\nu V^* + \epsilon E^* + \gamma I^* + \varphi Q^*}{\mu}. \end{cases}$$

□

A2. Proof of Theorem 2. According to System (1) and Eq. (2), the Jacobian matrix at the worm-free equilibrium P_0 is

$$J(P_0) = \begin{pmatrix} -(\sigma\nu+\mu) & 0 & -\dfrac{(1-\sigma\nu)\beta\Lambda}{\sigma\nu+\mu} & 0 & 0 \\ 0 & -(\eta+\epsilon+\mu) & \dfrac{(1-\sigma\nu)\beta\Lambda}{\sigma\nu+\mu} & 0 & 0 \\ 0 & \eta & -(\xi+\gamma+\mu+\theta) & 0 & 0 \\ 0 & 0 & \xi & -(\varphi+\mu+\theta) & 0 \\ \sigma\nu & \epsilon & \gamma & \varphi & -\mu \end{pmatrix},$$

and its characteristic equation is

$$\begin{aligned} |\lambda\mathbf{I} - J(P_0)| &= \begin{vmatrix} \lambda+\sigma\nu+\mu & 0 & \dfrac{(1-\sigma\nu)\beta\Lambda}{\sigma\nu+\mu} & 0 & 0 \\ 0 & \lambda+\eta+\epsilon+\mu & -\dfrac{(1-\sigma\nu)\beta\Lambda}{\sigma\nu+\mu} & 0 & 0 \\ 0 & -\eta & \lambda+\xi+\gamma+\mu+\theta & 0 & 0 \\ 0 & 0 & -\xi & \lambda+\varphi+\mu+\theta & 0 \\ -\sigma\nu & -\epsilon & -\gamma & -\varphi & \lambda+\mu \end{vmatrix} \\ &= (\lambda+\mu)(\lambda+\sigma\nu+\mu)(\lambda+\varphi+\mu+\theta)\left[(\lambda+\eta+\epsilon+\mu)(\lambda+\xi+\gamma+\mu+\theta) - \frac{(1-\sigma\nu)\beta\eta\Lambda}{\sigma\nu+\mu}\right] \\ &= 0. \end{aligned}$$

Obviously, Jacobian matrix $J(P_0)$ has three negative eigenvalues $\lambda_1 = -\mu$, $\lambda_2 = -(\sigma\nu+\mu)$, and $\lambda_3 = -(\varphi+\mu+\theta)$; the other eigenvalues of $J(P_0)$ are determined by the following equation:

$$\lambda^2 + (2\mu+\eta+\epsilon+\xi+\gamma+\theta)\lambda + (\eta+\epsilon+\mu)(\xi+\gamma+\mu+\theta) - \frac{(1-\sigma\nu)\beta\eta\Lambda}{\sigma\nu+\mu} = 0. \tag{A.11}$$

When $R_0 > 1$, we have $(\eta+\epsilon+\mu)(\xi+\gamma+\mu+\theta) - \frac{(1-\sigma\nu)\beta\eta\Lambda}{\sigma\nu+\mu} < 0$, which implies that Eq. (A.11) has both positive and negative roots. Therefore, the worm-free equilibrium P_0 is unstable saddle point. Otherwise, when $R_0 \le 1$, then by Hurwitz criterion [47], all roots of Eq. (A.11) have negative real parts, and so all eigenvalues of $J(P_0)$ have negative real parts. Then, using the stability theory [48], when $R_0 \le 1$, the worm-free equilibrium P_0 is locally asymptotically stable, which completes the proof. □

A3. Proof of Theorem 3. From the first equation of system (1), it follows that

$$V'(t) \le \Lambda - (\sigma\nu+\mu)V,$$

and by a simple computation, we have

$$V(t) \le \frac{e^{-(\sigma\nu+\mu)t} + \Lambda}{\sigma\nu+\mu},$$

which yields that, as $t \to \infty$,

$$V(t) \le \frac{\Lambda}{\sigma\nu+\mu} = V_0. \tag{A.12}$$

Consider the Lyapunov function as

$$L(E, I) = \eta E + (\eta+\mu+\epsilon)I.$$

Then, the derivative of $L(E, I)$ with respective to t gives

$$\begin{aligned}\frac{dL(E,I)}{dt} &= \eta E'(t) + (\eta+\epsilon+\mu)I'(t)\\ &= \eta\left[\frac{(1-\sigma\nu)\beta VI}{1+\alpha I} - (\eta+\epsilon+\mu)E\right] + (\eta+\epsilon+\mu)[\eta E - (\xi+\gamma+\mu+\theta)I]\\ &= \left[\frac{(1-\sigma\nu)\beta\eta V}{1+\alpha I} - (\eta+\epsilon+\mu)(\xi+\gamma+\mu+\theta)\right]I\\ &\le [(1-\sigma\nu)\beta\eta V_0 - (\eta+\epsilon+\mu)(\xi+\gamma+\mu+\theta)]I\\ &= \frac{(1-\sigma\nu)\beta\eta V_0}{R_0}(R_0-1)I,\end{aligned}$$

where the second last step is due to (A.12). Hence when $R_0 \le 1$, $\frac{dL(E,I)}{dt}$ is negative semi-definite.

Furthermore, $\frac{dL(E,I)}{dt} = 0$ if and only if $I = 0$. In fact, if $\frac{dL(E,I)}{dt} = 0$, then

$$\left[\frac{(1-\sigma\nu)\beta\eta V}{1+\alpha I} - (\eta+\epsilon+\mu)(\xi+\gamma+\mu+\theta)\right]I = 0,$$

and consequently either $I = 0$ or $V = \frac{(\eta+\epsilon+\mu)(\xi+\gamma+\mu+\theta)(1+\alpha I)}{(1-\sigma\nu)\beta\eta}$. For the second case, we show that, when $R_0 < 1$,

$$0 = V'(t) = \Lambda\left(1-\frac{1}{R_0}\right) - \frac{(\eta+\epsilon+\mu)(\xi+\gamma+\mu+\theta)}{\eta}\left[1+\frac{\alpha(\sigma\nu+\mu)}{(1-\sigma\nu)\beta}\right]I < 0,$$

which is a contradiction. On the other hand, if $I = 0$ then $0 = I'(t) = \eta E$, and consequently $E = 0$. Hence, when $R_0 \le 1$, the largest compact invariant set in $\{(E, I) \in \Omega | \dot{L}(E, I) = 0\}$ is a singleton containing the origin. Moreover, it follows from (A.12) that $\lim_{t\to\infty}(V(t), E(t), I(t), Q(t), S(t)) = P_0$, and applying the LaSalles invariance principle [49], the worm-free equilibrium P_0 is globally asymptotically stable in Ω when $R_0 \le 1$.

When $R_0 > 1$, we have $\frac{dL(E,I)}{dt} > 0$ for V sufficiently close to $\frac{\Lambda}{\sigma\nu+\mu}$ except when $E = I = 0$. Solutions starting sufficiently close to P_0 leave a neighborhood of P_0 except those on the invariant V-axis, on which (1) reduces to $V' = \Lambda - (\sigma\nu+\mu)V$, and then $V(t) \to \frac{\Lambda}{\sigma\nu+\mu}$ as $t \to \infty$. □

It is pointed out here that the unstable property of the worm-free equilibrium P_0 when $R_0 > 1$ can also be derived by the eigenvalue analysis in Appendix A2.

A4. Proof of Theorem 4. Considering that P_0 is unstable if $R_0 > 1$ and $P_0 \in \partial\Omega$, we prove from Theorem 4.3 of [50] that system (1) is uniform persistent in Ω if and only if $R_0 > 1$. □

A5. Proof of Theorem 5. According to $P^* = (V^*, E^*, I^*, Q^*, S^*)$ with its coordinates satisfying (4), the Jacobian matrix of system (1) at the worm-existence equilibrium P^* is

$$J(P^*) = \begin{pmatrix} -\frac{(1-\sigma\nu)\beta I^*}{1+\alpha I^*} - (\sigma\nu+\mu) & 0 & -\frac{(1-\sigma\nu)\beta V^*}{(1+\alpha I^*)^2} & 0 & 0\\ \frac{(1-\sigma\nu)\beta I^*}{1+\alpha I^*} & -(\eta+\epsilon+\mu) & \frac{(1-\sigma\nu)\beta V^*}{(1+\alpha I^*)^2} & 0 & 0\\ 0 & \eta & -(\xi+\gamma+\mu+\theta) & 0 & 0\\ 0 & 0 & \xi & -(\varphi+\mu+\theta) & 0\\ \sigma\nu & \epsilon & \gamma & \varphi & -\mu \end{pmatrix}.$$

The characteristic equation of the above matrix is

$$\begin{aligned}|\lambda\mathbf{I} - J(P^*)| &= \begin{vmatrix} \lambda + \frac{(1-\sigma\nu)\beta I^*}{1+\alpha I^*} + \sigma\nu + \mu & 0 & \frac{(1-\sigma\nu)\beta V^*}{(1+\alpha I^*)^2} & 0 & 0\\ -\frac{(1-\sigma\nu)\beta I^*}{1+\alpha I^*} & \lambda+\eta+\epsilon+\mu & -\frac{(1-\sigma\nu)\beta V^*}{(1+\alpha I^*)^2} & 0 & 0\\ 0 & -\eta & \lambda+\xi+\gamma+\mu+\theta & 0 & 0\\ 0 & 0 & -\xi & \lambda+\varphi+\mu+\theta & 0\\ -\sigma\nu & -\epsilon & -\gamma & -\varphi & \lambda+\mu \end{vmatrix}\\ &= (\lambda+\mu)(\lambda+\varphi+\mu+\theta)\left\{(\lambda+\eta+\epsilon+\mu)(\lambda+\xi+\gamma+\mu+\theta)\left[\lambda+\sigma\nu+\mu+\frac{(1-\sigma\nu)\beta I^*}{1+\alpha I^*}\right]\right.\end{aligned}$$

$$-\frac{(1-\sigma\nu)\beta\eta V^*}{(1+\alpha I^*)^2}\left[\lambda+\sigma\nu+\mu+\frac{(1-\sigma\nu)\beta I^*}{1+\alpha I^*}\right]+\frac{(1-\sigma\nu)^2\beta^2\eta V^* I^*}{(1+\alpha I^*)^3}\Bigg\}$$
$$=0.$$

It is obvious that the matrix $J(P^*)$ has two negative eigenvalues $\lambda_1=-\mu$, and $\lambda_2=-(\varphi+\mu+\theta)$. Therefore, we only need to consider the roots of the following equation:

$$\lambda^3+B_1\lambda^2+B_2\lambda+B_3=0, \tag{A.13}$$

where

$$B_1=\eta+\epsilon+\xi+\gamma+\theta+3\mu+\sigma\nu+\frac{(1-\sigma\nu)\beta I^*}{1+\alpha I^*},$$
$$B_2=(\eta+\epsilon+\xi+\gamma+\theta+2\mu)\left[\sigma\nu+\mu+\frac{(1-\sigma\nu)\beta I^*}{1+\alpha I^*}\right]+(\eta+\epsilon+\mu)(\xi+\gamma+\mu+\theta)-\frac{(1-\sigma\nu)\beta\eta V^*}{(1+\alpha I^*)^2},$$

and

$$B_3=\frac{(1-\sigma\nu)\beta I^*}{1+\alpha I^*}(\eta+\epsilon+\mu)(\xi+\gamma+\mu+\theta)+(\sigma\nu+\mu)\left[(\eta+\epsilon+\mu)(\xi+\gamma+\mu+\theta)-\frac{(1-\sigma\nu)\beta\eta V^*}{(1+\alpha I^*)^2}\right].$$

Clearly, $B_1>0$; and based on the following relation

$$\frac{(1-\sigma\nu)\beta\eta V^*}{1+\alpha I^*}=(\eta+\epsilon+\mu)(\xi+\gamma+\mu+\theta),$$

we have that $B_2>0$ and $B_3>0$. Further by a direct computation, we show that $B_1B_2-B_3>0$. Then by the Hurwitz criterion [47], all roots of Eq. (A.13) have negative real parts, and so all eigenvalues of $J(P^*)$ have negative real parts. Hence by the stability theory [48], the worm-existence equilibrium P^* is locally asymptotically stable with respect to Ω when $R_0>1$. □

A6. Proof of Theorem 6. We now prove Theorem 6 by using the Li–Muldowney geometric approach, where we omit the detailed introduction of this approach and refer readers to [35].

Firstly, we deal with the sub-system of (1):

$$\begin{cases} V'(t)=\Lambda-\dfrac{(1-\sigma\nu)\beta VI}{1+\alpha I}-(\sigma\nu+\mu)V,\\ E'(t)=\dfrac{(1-\sigma\nu)\beta VI}{1+\alpha I}-(\eta+\epsilon+\mu)E,\\ I'(t)=\eta E-(\xi+\gamma+\mu+\theta)I. \end{cases} \tag{A.14}$$

The Jacobian matrix of system (A.14) is

$$J=\begin{pmatrix} -\dfrac{(1-\sigma\nu)\beta I}{1+\alpha I}-(\sigma\nu+\mu) & 0 & -\dfrac{(1-\sigma\nu)\beta V}{(1+\alpha I)^2}\\ \dfrac{(1-\sigma\nu)\beta I}{1+\alpha I} & -(\eta+\epsilon+\mu) & \dfrac{(1-\sigma\nu)\beta V}{(1+\alpha I)^2}\\ 0 & \eta & -(\xi+\gamma+\mu+\theta) \end{pmatrix}$$

and its second additive compound matrix is

$$J^{[2]}=\begin{pmatrix} -\dfrac{(1-\sigma\nu)\beta I}{1+\alpha I}-m & \dfrac{(1-\sigma\nu)\beta V}{(1+\alpha I)^2} & \dfrac{(1-\sigma\nu)\beta V}{(1+\alpha I)^2}\\ \eta & -\dfrac{(1-\sigma\nu)\beta I}{1+\alpha I}-n & 0\\ 0 & \dfrac{(1-\sigma\nu)\beta I}{1+\alpha I} & -k \end{pmatrix},$$

where $m=\sigma\nu+\eta+\epsilon+2\mu$, $n=\sigma\nu+\xi+\gamma+\theta+2\mu$, and $k=\eta+\epsilon+\xi+\gamma+\theta+2\mu$. Define a function $A=A(V,E,I)=\mathrm{diag}(1,\frac{E}{I},\frac{E}{I})$, we obtain its directional derivative along (V,E,I) as

$$A_f=\mathrm{diag}\left(0,\frac{E'I-I'E}{I^2},\frac{E'I-I'E}{I^2}\right).$$

Then,

$$A_fA^{-1}=\mathrm{diag}\left(0,\frac{E'}{E}-\frac{I'}{I},\frac{E'}{E}-\frac{I'}{I}\right),$$

and

$$AJ^{[2]}A^{-1} = \begin{pmatrix} -\frac{(1-\sigma\nu)\beta I}{1+\alpha I} - m & \frac{(1-\sigma\nu)\beta VI}{E(1+\alpha I)^2} & \frac{(1-\sigma\nu)\beta VI}{E(1+\alpha I)^2} \\ \frac{\eta E}{I} & -\frac{(1-\sigma\nu)\beta I}{1+\alpha I} - n & 0 \\ 0 & \frac{(1-\sigma\nu)\beta I}{1+\alpha I} & -k \end{pmatrix}.$$

Set $B = A_f A^{-1} + AJ^{[2]}A^{-1}$, which can be written in matrix form:

$$B = \begin{pmatrix} B_{11} & B_{12} \\ B_{21} & B_{22} \end{pmatrix},$$

with

$$B_{11} = -\frac{(1-\sigma\nu)\beta I}{1+\alpha I} - m,$$

$$B_{12} = \left(\frac{(1-\sigma\nu)\beta VI}{E(1+\alpha I)^2}, \frac{(1-\sigma\nu)\beta VI}{E(1+\alpha I)^2} \right),$$

$$B_{21} = \left(\frac{\eta E}{I}, 0 \right)^T,$$

$$B_{22} = \begin{pmatrix} \frac{E'}{E} - \frac{I'}{I} - \frac{(1-\sigma\nu)\beta I}{1+\alpha I} - n & 0 \\ \frac{(1-\sigma\nu)\beta I}{1+\alpha I} & \frac{E'}{E} - \frac{I'}{I} - k \end{pmatrix}.$$

Let (u, v, w) be a vector in $\mathbb{R}^3$ with its norm defined by

$$||(u, v, w)|| = \max\{|u|, |v| + |w|\}.$$

Let $\mu(B)$ be the *Lozinskiĭ* measure with respect to this norm. Then as described in [51], we choose

$$\mu(B) \le \sup\{g_1, g_2\},$$

where $g_1 = \mu_1(B_{11}) + |B_{12}|$, $g_2 = |B_{21}| + \mu_1(B_{22})$, $|B_{12}|$, $|B_{21}|$ are matrix norms with respect to the l_1 vector norm, and μ_1 is the *Lozinskiĭ* measure with respect to l_1 norm. As a result, we get

$$\mu_1(B_{11}) = -\frac{(1-\sigma\nu)\beta I}{1+\alpha I} - m, \quad |B_{21}| = \frac{\eta E}{I}, \quad |B_{12}| = \frac{(1-\sigma\nu)\beta VI}{E(1+\alpha I)^2},$$

and

$$\mu_1(B_{22}) = \max\left\{ \frac{E'}{E} - \frac{I'}{I} - n, \frac{E'}{E} - \frac{I'}{I} - k \right\} = \frac{E'}{E} - \frac{I'}{I} - \min\{n, k\}.$$

Therefore,

$$g_1 = -\frac{(1-\sigma\nu)\beta I}{1+\alpha I} - m + \frac{(1-\sigma\nu)\beta VI}{E(1+\alpha I)^2},$$

and

$$g_2 = \frac{\eta E}{I} + \frac{E'}{E} - \frac{I'}{I} - \min\{n, k\}.$$

From (A.14), we have

$$\frac{E'}{E} = \frac{(1-\sigma\nu)\beta VI}{E(1+\alpha I)} - (\eta + \epsilon + \mu),$$

and

$$\frac{I'}{I} = \frac{\eta E}{I} - (\xi + \gamma + \mu + \theta).$$

Then,

$$g_1 = -\frac{(1-\sigma\nu)\beta I}{1+\alpha I} - m + \frac{(1-\sigma\nu)\beta VI}{E(1+\alpha I)} + \left[\frac{(1-\sigma\nu)\beta VI}{E(1+\alpha I)^2} - \frac{(1-\sigma\nu)\beta VI}{E(1+\alpha I)} \right]$$

$$= \frac{E'}{E} - \mu - \frac{(1-\sigma\nu)\beta VI}{(1+\alpha I)} - \sigma\nu + \left[\frac{(1-\sigma\nu)\beta VI}{E(1+\alpha I)^2} - \frac{(1-\sigma\nu)\beta VI}{E(1+\alpha I)}\right]$$
$$\leq \frac{E'}{E} - \mu,$$

and

$$g_2 = \frac{E'}{E} + (\xi + \gamma + \mu + \theta) - \min\{n, k\}$$
$$= \frac{E'}{E} - \mu - \min\{\sigma\nu, \eta + \epsilon\}$$
$$\leq \frac{E'}{E} - \mu.$$

Further, we obtain

$$\mu(B) \leq \sup\{g_1, g_2\} \leq \frac{E'}{E} - \mu.$$

In the light of the fact that there exists a sufficiently large $T > 0$ such that for all $t > T$, $\frac{E(t)}{E(0)} < e^{\frac{\mu t}{2}}$; namely, $\frac{1}{t}\ln\frac{E(t)}{E(0)} < \frac{\mu}{2}$, it follows that for all $t > T$,

$$\frac{1}{t}\int_0^t \mu(B)ds \leq \frac{1}{t}\int_0^t \left(\frac{E'}{E} - \mu\right)ds = \frac{1}{t}\ln\frac{E(t)}{E(0)} - \mu < -\frac{\mu}{2},$$

which leads to

$$q = \limsup_{t\to\infty} \sup_{(V(0),E(0),I(0))\in \mathrm{int}(\Omega)} \frac{1}{t}\int_0^t \mu(B)ds \leq -\frac{\mu}{2} < 0.$$

Hence by Theorem 3.5 of [35], the worm-existence equilibrium (V^*, E^*, I^*) is globally asymptotically stable.

Next, we consider the following sub-system of system (1):

$$\begin{cases} Q'(t) = \xi I - (\varphi + \mu + \theta)Q, \\ S'(t) = \sigma\nu V + \epsilon E + \gamma I + \varphi Q - \mu S. \end{cases} \tag{A.15}$$

The limit system of (A.15) is

$$\begin{cases} Q'(t) = \xi I^* - (\varphi + \mu + \theta)Q, \\ S'(t) = \sigma\nu V^* + \epsilon E^* + \gamma I^* + \varphi Q - \mu S. \end{cases}$$

Then, we get

$$\begin{cases} Q(t) = e^{-(\varphi+\mu+\theta)t}\left[Q(0) + \xi I^* \int_0^t e^{(\varphi+\mu+\theta)s}ds\right], \\ S(t) = e^{-\mu t}\left[S(0) + \int_0^t [\sigma\nu V^* + \epsilon E^* + \gamma I^* + \varphi Q(s)]e^{\mu s}ds\right], \end{cases}$$

which implies that, as $t \to \infty$,

$$Q(t) \to \frac{\xi I^*}{\varphi + \mu + \theta} = Q^*, \quad \text{and} \quad R(t) \to \frac{\sigma\nu V^* + \epsilon E^* + \gamma I^* + \varphi Q^*}{\mu} = S^*.$$

Consequently, the worm-existence equilibrium P^* is globally asymptotically stable in $\mathrm{int}(\Omega)$ when $R_0 > 1$, which completes the proof. □

A7. Proof of Theorem 7. To prove the existence of an optimal control pair, it is easy to verify that

1. Since the state system (5) has bounded coefficient, the set of controls and corresponding state variables is nonempty.
2. Note that the solution of system (5) are bounded, the control set U is convex and closed.
3. Since the state system (5) is bilinear in u_1 and u_2, the right hand side of (5) is bounded by a linear function in the state and control variables, where we use the boundedness of these solutions.
4. The integrand of the objective cost function, $Ku_1^2(t) + Lu_2^2(t) + E(t) + I(t) - S(t)$, is clearly convex on U.
5. There exists constants $c_1 > 0$, $c_2 > 0$, and $\pi > 1$ such that the integrand of the objective cost function satisfying

$$Ku_1^2(t) + Lu_2^2(t) + E(t) + I(t) - S(t) \geq c_1(|u_1|^2 + |u_2|^2)^{\pi/2} - c_2,$$

where c_2 depends on the boundedness of $E(t)$, $I(t)$ and $S(t)$, and $c_1 > 0$ is due to $K > 0$ and $L > 0$.

Hence, the existence of optimal control pair follows directly from Fleming and Rishel [45]. □

A8. Proof of Theorem 8. The expression of adjoint equations and boundary conditions are standard results from Pontryagin's Minimum Principle [44]. By the differentiating the Hamiltonian (7) with respective to respective states, the adjoint equations can be written as (8) with boundary conditions $w_i(t_f) = 0$, for $i = 1, \ldots, 5$.

By using the optimal conditions, the unrestricted optimal control pair (u_1^*, u_2^*) satisfy

$$\frac{\partial H}{\partial u_1^*} = \frac{\partial H}{\partial u_2^*} = 0. \tag{A.16}$$

Note that

$$H = Ku_1^2 + \frac{(w_1 - w_2)u_1\beta VI}{1+\alpha I} + (w_5 - w_1)u_1 V + Lu_2^2 + (w_4 - w_3)u_2 I + \text{ other terms without } u_1 \text{ and } u_2,$$

which, along with (A.16), leads to

$$\begin{cases} \dfrac{\partial H}{\partial u_1^*} = 2Ku_1^* + \dfrac{(w_1 - w_2)\beta VI}{1+\alpha I} + (w_5 - w_1)V = 0, \\ \dfrac{\partial H}{\partial u_2^*} = 2Lu_2^* + (w_4 - w_3)I = 0. \end{cases}$$

Thus, we have

$$\begin{cases} u_1^* = \dfrac{1}{2K}\left[\dfrac{(w_2 - w_1)\beta VI}{1+\alpha I} + (w_1 - w_5)V\right], \\ u_2^* = \dfrac{(w_3 - w_4)I}{2L}. \end{cases}$$

Because of the boundedness of the standard control, we derive for the control u_1^* that

$$u_1^* = \begin{cases} 0, & \dfrac{1}{2K}\left[\dfrac{(w_2 - w_1)\beta VI}{1+\alpha I} + (w_1 - w_5)V\right] \le 0; \\ \dfrac{1}{2K}\left[\dfrac{(w_2 - w_1)\beta VI}{1+\alpha I} + (w_1 - w_5)V\right], & 0 < \dfrac{1}{2K}\left[\dfrac{(w_2 - w_1)\beta VI}{1+\alpha I} + (w_1 - w_5)V\right] < 1; \\ 1, & \dfrac{1}{2K}\left[\dfrac{(w_2 - w_1)\beta VI}{1+\alpha I} + (w_1 - w_5)V\right] \ge 1. \end{cases}$$

Hence, the compact form of u_1^* is

$$u_1^* = \max\left\{0, \min\left\{1, \frac{1}{2K}\left[\frac{(w_2 - w_1)\beta VI}{1+\alpha I} + (w_1 - w_5)V\right]\right\}\right\}.$$

Similarly, the control u_2^* has the compact form as

$$u_2^* = \max\left\{0, \min\left\{1, \frac{(w_3 - w_4)I}{2L}\right\}\right\}.$$

Therefore, the proof of this theorem is completed. □

A9. Proof of Corollary 1. From Eq. (3), we have that $R_0 < 1$ if and only if

$$\frac{(1 - \sigma\nu)\beta\eta\Lambda}{(\sigma\nu + \mu)(\eta + \epsilon + \mu)(\xi + \gamma + \mu + \theta)} < 1,$$

which, along with Theorems 2 and 3, shows that the worm outbreak does not become epidemic iff

$$(1 - \sigma\nu)\beta\eta\Lambda < (\sigma\nu + \mu)(\eta + \epsilon + \mu)(\xi + \gamma + \mu + \theta).$$

Since $\eta < \eta + \epsilon + \mu$, we have $R_0 < 1$ if

$$\Lambda < \frac{(\sigma\nu + \mu)(\xi + \gamma + \mu + \theta)}{(1 - \sigma\nu)\beta}.$$

Using the similar derivation as above, we can get the results for the other parameters. □

References

[1] D. Moore, V. Paxson, S. Savage, C. Shannon, S. Staniford, N. Weaver, Inside the slammer worm, IEEE Mag. Secur. Privacy 1 (4) (2003) 33–39.
[2] M.L. Polla, F. Martinelli, D. Sgandurra, A survey on security for mobile devices, IEEE Commun. Surv. Tutor. 15 (1) (2013) 446–471.
[3] W. Xia, Z. Li, Z. Chen, Z. Yuan, Cornmwarrior worm propagation model for smart phone networks, J. Chin. Univ. Posts Telecommun. 15 (2) (2008) 60–66.
[4] J. Jamaluddin, N. Zotou, P. Coulton, Mobile phone vulnerabilities: a new generation of malware, Proceedings of IEEE International Symposium on Consumer Electronics (2004) 199–202.
[5] S. Peng, S. Yu, A. Yang, Smartphone malware and its propagation modeling: a survey, IEEE Commun. Surv. Tutor. 16 (2) (2014) 925–941.
[6] J. Scharr, New WiFi Worm can Spread Like an Airborne Disease, 2014, https://wwww.yahoo.com/tech/new-wifi-worm-can-read-like-an-airborne-disease-78496514830.html.
[7] S. Peng, A survey on malware containment models in smartphones, Appl. Mech. Mater. 263–266 (2013) 3005–3011.
[8] K. Haldar, B.K. Mishra, A mathematical model for a distributed attack on targeted resources in a computer network, Commun. Nolinear Sci. Numer. Simul. 19 (9) (2014) 3149–3160.
[9] J.D.H. Guilln, A.M. del Rey, L.H. Encinas, Study of the stability of a SEIRS model for computer worm propagation, Physica A 479 (2017) 411–421.
[10] J.D.H. Guilln, A.M. del Rey, Modeling malware propagation using a carrier compartment, Commun. Nolinear Sci. Numer. Simul. 56 (2018) 217–226.
[11] O.A. Toutonji, S.M. Yoo, M. Park, Stability analysis of VEISV propagation modeling for network worm attack, Appl. Math. Model. 36 (2012) 2751–2761.
[12] Q. Zhu, X. Yang, J. Ren, Modeling and analysis of the spread of computer virus, Commun. Nolinear Sci. Numer. Simul. 17 (2012) 5117–5124.
[13] C.C. Zou, W. Gong, D. Towsley, Worm propagation modeling and analysis under dynamic quarantine defense, in: Proceedings of the 2003 ACM Workshop on Rapid Malcode (WORM'03), 2003, pp. 51–60.
[14] O.A. Toutonji, S.M. Yoo, Passive benign worm propagation modeling with dynamic quarantine defense, KSII Trans. Internet Inf. Syst. 3 (1) (2009) 96–107.
[15] F.W. Wang, Y.K. Zhang, C.G. Wand, J.F. Ma, S.J. Moon, Stability analysis of a SEIQV epidemic model for rapid spreading worms, Comput. Secur. 29 (2010) 410–418.
[16] X. Liu, L. Yang, Stability analysis of an SEIQV epidemic model with saturated incidence rate, Nolinear Anal. RWA 13 (2012) 2671–2679.
[17] B.K. Mishra, N. Jha, SEIQRS model for the transmission of malicious objects in computer network, Appl. Math. Model. 34 (2010) 710–715.
[18] X. Xiao, P. Fu, C. Dou, Q. Li, G. Hu, S. Xia, Design and analysis of SEIQR worm propagation model in mobile internet, Commun. Nolinear Sci. Numer. Simul. 43 (2017) 341–350.
[19] F. Fenner, D.A. Henderson, I. Arita, Z. Jezek, I.D. Ladnyi, Smallpox and its Eradication, WHO, 1998.
[20] M. De la Sen, A. Ibeas, S. Alonso-Quesada, On vaccination controls for the SEIR epidemic model, Commun. Nolinear Sci. Numer. Simul. 17 (2012) 2637–2658.
[21] X. Wang, H. Peng, B. Shi, D. Jiang, S. Zhang, B. Chen, Optimal vaccination strategy of a constrained time-varying SEIR epidemic model, Commun. Nolinear Sci. Numer. Simul. 67 (2019) 37–48.
[22] B.K. Mishra, S.K. Pandey, Dynamic model of worm propagation in computer network, Appl. Math. Model. 38 (2014) 2173–2179.
[23] C. Sun, Y.H. Hsieh, Global analysis of an SEIR model with varying population size and vaccination, Appl. Math. Model. 34 (2010) 2685–2697.
[24] L. Cai, X. Li, Analysis of a SEIV epidemic model with a nonlinear incidence rate, Appl. Math. Model. 33 (2009) 2919–2926.
[25] V. Capasso, G. Serio, A generation of the Kermack-Mckendrick deterministic epidemic model, Math. Biosci. 42 (1978) 43–61.
[26] J. Jian, J. Xiao, Stability analysis of a disease resistance SEIRS model with nonlinear incidence rate, Adv. Differ. Equ. 75 (2018), doi:10.1186/s13662-018-1494-1.
[27] C. Sun, Y. Lin, S. Tang, Global stability for an special SEIR epidemic model with nonlinear incidence rates, Chaos Solitons Fractals 33 (1) (2007) 290–297.
[28] L. Wang, Z. Liu, X. Zhang, Global dynamics of an SVEIR epidemic model with distributed delay and nonlinear incidence, Appl. Math. Comput. 284 (2016) 47–65.
[29] O. Diekmann, J.A.P. Heesterbeek, J.A.J. Metz, On the definition and the computation of the basic reproduction ratio r_0 in models for infectious diseases in heterogeneous populations, J. Math. Bio. 28 (4) (1990) 365–382.
[30] C. Liao, C. Chang, H. Liang, Probabilistic transmission dynamic model to assess indoor airborne infection risks, Risk Anal. 25 (5) (2005) 1097–1107.
[31] C. Castillo-Chavez, Z. Feng, W. Huang, On the computation of r_0 and its role on global stability, Inst. Math. Appl. 125 (2002) 229–255.
[32] X. Zhao, Dynamical systems in population biology, CMS Books in Mathematics, Canadian Mathematical Society, Springer, 2003.
[33] G. Butler, P. Waltman, Uniformly persistent systems, Proc. Am. Math. Soc. 96 (1986) 425–430.
[34] G.J. Butler, P. Waltman, Persistence in dynamical systems, J. Differ. Equ. 63 (1986) 255–263.
[35] M.Y. Li, J.S. Muldowney, A geometric approach to global-stability problems, SIAM J. Math. Anal. 27 (4) (1996) 1070–1083.
[36] C. Shannon, D. Moore. The Spread of the Code-red Worm. 2001, http://www.caida.org/analysis/security/code-red/coderedv2_analysis.xml.
[37] A.K. Roy, P.K. Roy, E. Grigorieva, Mathematical insights on psoriasis regaulation: role of th1 and th2 cells, Math. Biosci. Eng. 15 (3) (2018) 717–738.
[38] P.K. Roy, A.N. Chatterjee, Effect of HAART on CTL mediated immune cells: an optimal control theoretic approach, in: Electrical Engineering and Applied Computing, Springer, Dordrecht, 2011, pp. 595–607.
[39] A.N. Chatterjee, P.K. Roy, Anti-viral drug treatment along with immune activator IL-2: a control-based mathematical approach for HIV infection, Int. J. Control 85 (2) (2012) 220–237.
[40] S. Saha, P.K. Roy, A comparative study between two systems with and without awareness in controlling HIV/AIDS, Int. J. Appl. Math. Comput. Sci. 27 (2) (2017) 337–350.
[41] F.A. Basir, K.B. Blyuss, S. Ray, Modelling the effects of awareness-based interventions to control the mosaic disease of jatropha curcas, Ecol. Complex. 36 (2018) 92–100.
[42] X.H. Chang, R.R. Liu, J.H. Park, A further study on output feedback h_∞ control for discrete-time systems, IEEE Trans. Circuits Syst. II: Express Briefs 66 (3) (2018), doi:10.1109/TCSII.2019.2904320.
[43] X.H. Chang, G.H. Yang, New results on output feedback h_∞ control for linear discrete-time systems, IEEE Trans. Autom. Control 59 (5) (2014) 1355–1359.
[44] L.S. Pontryagin, V.G. Boltyanskii, R.V. Gamkrelidze, E.F. Mishchenko, Mathematical Theory of Optimal Processes, 4, Gordon and Breach Science Publishers, New York, London, 1986.
[45] W.H. Fleming, R.W. Rishel, Deterministic and Stochastic Optimal Control, Springer-Verlag, Berlin, New York, 1975.
[46] H.R. Joshi, Optimal control of an HIV immunology model, Optim. Control Appl. Methods 23 (2002) 199–213.
[47] A. Hurwitz, On the conditions under which an equation has only roots with negative real parts, in: R.T. Ballman, et al. (Eds.), Selected Papers on Mathematical Trends in Control Theory, Dover, New York, 1964.
[48] R.C. Robinson, An Introduction to Dynamical System: Continuous and Discrete, Prentice Hall, USA, 2004.
[49] J.P. La Salle, The stability of dynamical systems, in: Proceedings of Regional Conference Series in Applied Mathematics, 25, Society for Industrial and Applied Mathematics, Philadelphia, 1976.
[50] H.I. Freedman, S.G. Ruan, M. Tang, Uniform persistence and flows near a closed positively invariant set, J. Dyn. Differ. Equ. 6 (4) (1994) 583–600.
[51] J.R. Martin, Logarithmic norms and projections applied to linear differential systems, J. Math. Anal. Appl. 45 (1974) 432–454.